Cosmological long-wavelength solutions and primordial black hole formation

Tomohiro Harada,[1,*] Chul-Moon Yoo,[2,†] Tomohiro Nakama,[3,‡] and Yasutaka Koga[1,§]

[1]*Department of Physics, Rikkyo University, Toshima, Tokyo 171-8501, Japan*
[2]*Gravity and Particle Cosmology Group, Division of Particle and Astrophysical Science,*
Graduate School of Science, Nagoya University, Furo-cho, Chikusa-ku, Nagoya 464-8602, Japan
[3]*Research Center for the Early Universe (RESCEU), Graduate School of Science, University of Tokyo,*
Bunkyo-ku, Tokyo 113-0033, Japan

We construct cosmological long-wavelength solutions without symmetry in general gauge conditions which are compatible with the long-wavelength scheme. We then specify the relationship among the solutions in different time slicings. Nonspherical long-wavelength solutions are particularly important for primordial structure formation in the epoch of very soft equations of state. Applying this general framework to spherical symmetry, we show the equivalence between long-wavelength solutions in the constant mean curvature slicing with conformally flat spatial coordinates and asymptotic quasihomogeneous solutions in the comoving slicing with the comoving threading. We derive the correspondence relation between these two solutions and compare the results of numerical simulations of primordial black hole (PBH) formation in these two different approaches. To discuss the PBH formation, it is convenient and conventional to use $\tilde{\delta}_c$, the value which the averaged density perturbation at threshold in the comoving slicing would take at horizon entry in the lowest-order long-wavelength expansion. We numerically find that within (approximately) compensated models, the sharper the transition from the overdense region to the Friedmann-Robertson-Walker universe is, the larger the $\tilde{\delta}_c$ becomes. We suggest that, for the equation of state $p = (\Gamma - 1)\rho$, we can apply the analytic formulas for the minimum $\tilde{\delta}_{c,\mathrm{min}} \simeq [3\Gamma/(3\Gamma + 2)]\sin^2[\pi\sqrt{\Gamma - 1}/(3\Gamma - 2)]$ and the maximum $\tilde{\delta}_{c,\mathrm{max}} \simeq 3\Gamma/(3\Gamma + 2)$. As for the threshold peak value of the curvature variable $\psi_{0,c}$, we find that the sharper the transition is, the smaller the $\psi_{0,c}$ becomes. We analytically explain this intriguing feature qualitatively with a compensated top-hat density model. Using simplified models, we also analytically deduce an environmental effect that $\psi_{0,c}$ can be significantly larger (smaller) if the underlying perturbation of much longer wavelength is positive (negative).

I. INTRODUCTION

The proposal that black holes may have formed in the early Universe, which are called primordial black holes (PBHs), has recently been extensively studied in cosmology because they can convey unique information about the early Universe to us. This is because energy scales relevant to PBHs are generally very different from those of the observed cosmic microwave background anisotropy. The possibility of PBHs has been indicated by Zeldovich and Novikov [1] and Hawking [2]. Since PBHs evaporate by emitting radiation and they also act as gravitational sources before they evaporate away, current observations constrain the abundance of PBHs using the big bang nucleosynthesis, extragalactic photon background and gravitational and astrophysical effects of nonevaporating PBHs [3,4]. To convert the observed abundance of PBHs to the information

of the early Universe, the key issues are the production efficiency of PBHs from given cosmological perturbations and the time evolution of PBHs through mass accretion and Hawking evaporation [1,3,5].

Here, we focus on the criterion of PBH formation. Since the probability of PBH formation is expected to be exponentially small, the abundance of PBHs for given perturbations is sensitive to the formation criterion. As a pioneer, Carr [3] derived $\delta_c \simeq \Gamma - 1$ for the equation of state $p = (\Gamma - 1)\rho$ almost in an order-of-magnitude estimate, where δ_c is the threshold value of the density perturbation at horizon entry. This gives $\delta_c \simeq 1/3$ for a radiation fluid $\Gamma = 4/3$. In fact, it turns out that it is not so straightforward to accurately determine the formation criterion of PBHs as we have to understand highly general relativistic nonlinear dynamics in the cosmological background. Recently, numerical relativity has developed so much that the formation of PBHs can be simulated and the threshold of PBH formation can be obtained [6–16]. Shibata and Sasaki [9] gave the threshold $\psi_{0,c} \simeq 1.4$–1.8, where $\psi_{0,c}$ is the threshold value of the peak value ψ_0 of the curvature variable ψ and

*harada@rikkyo.ac.jp
†yoo@gravity.phys.nagoya-u.ac.jp
‡nakama@resceu.s.u-tokyo.ac.jp
§koga@rikkyo.ac.jp

this is consistent with $\delta_c \simeq 0.3$–0.5 [17,18]. Polnarev and Musco [11] gave $\tilde{\delta}_c \simeq 0.45$–$0.66$ for a radiation fluid, depending on the perturbation profiles, where $\tilde{\delta}_c$ is the threshold value of the averaged density perturbation δ_c at horizon entry in the comoving slicing in the lowest-order long-wavelength expansion. Musco and Miller [13] gave $\tilde{\delta}_c$ for different values of Γ. Nakama *et al.* [15] investigated the PBH formation threshold for a much wider class of initial curvature perturbation profiles characterized by five parameters. Harada *et al.* [19] derived an analytic formula $\tilde{\delta}_c = [3\Gamma/(3\Gamma+2)]\sin^2[\pi\sqrt{\Gamma-1}/(3\Gamma-2)]$ under a certain set of assumptions, which gives $\tilde{\delta}_c \simeq 0.4135$ for a radiation fluid. Young *et al.* [18] suggested that there is a significant environmental effect on $\psi_{0,c}$ but not on $\tilde{\delta}_c$. Very recently, Tada and Yokoyama [20] and Young and Byrnes [21] have found that the PBH production rate is significantly biased if the statistics of the primordial curvature perturbation has small local-type non-Gaussianity.

To discuss the PBH formation or any other primordial structure formation, it is important to give cosmological perturbations which can be generated in the early Universe. On the other hand, the initial data set which will result in PBH formation must nonlinearly deviate from the Friedmann-Robertson-Walker (FRW) universe even much before the horizon entry of the scale of the perturbations. Such cosmological primordial perturbations are formulated by Lyth *et al.* [22]. There have been two approaches so far in which the appropriate initial data of cosmological perturbations are prepared and the Einstein equations are numerically solved in spherical symmetry to follow the formation of PBHs. The one is initiated by Shibata and Sasaki [9] and the other is by Polnarev and Musco [11]. Although these two approaches study the same problem, the direct comparison of their results has not been done, and for this reason the complete picture of PBH formation has yet been unclear.

In this paper, without assuming symmetry, we construct cosmological long-wavelength solutions which can deviate from the FRW spacetimes with an arbitrarily large amplitude and are naturally generated in inflationary cosmology. These solutions can be applied as the initial data for PBH formation and any other primordial structure formation in spherical symmetry or in nonspherical situations. Nonspherical cosmological perturbations should be particularly important for PBH formation in the stage when the effective equation of state is very soft [23,24,25]. Such stages have recently been discussed in some scenarios of inflationary cosmology [26–29].

We explicitly show that the solutions in spherical symmetry reduce to the ones in Shibata and Sasaki [9] in some gauge and to the ones in Polnarev and Musco [11] in another gauge. Thus, we derive the correspondence relation between these two approaches. Based on this correspondence relation, we compare the numerical results obtained in these two approaches and find that the results are consistent. We analyze three different measures of the amplitude of perturbations, $\tilde{\delta}$, ψ_0, and the maximum value of the compaction function $\mathcal{C}_{\max}$. The threshold values of these three quantities depend on the initial density (or curvature) profiles. We analyze how the threshold values depend on the profiles and physically understand the dependence using simplified models. We also discuss an environmental or bias effect on $\psi_{0,c}$ when perturbations are superimposed on perturbations of longer wavelength.

This paper is organized as follows. In Sec. II, we present the $3+1$ formulation of the Einstein equations and the cosmological conformal decomposition. In Sec. III, we review the long-wavelength scheme. In Sec. IV, we present the long-wavelength solutions in different gauge conditions. In Sec. V, we present the gauge conditions adopted in Shibata and Sasaki [9] and Polnarev and Musco [11] and find the relation among quasilocal quantities in spherical symmetry. In Sec. VI, we show the equivalence between the long-wavelength solutions obtained in the two approaches and derive the correspondence relation. In Sec. VII, we compare and interpret the numerical results obtained in the two approaches. In Sec. VIII, we discuss the environmental effect on $\psi_{0,c}$ with several simplified models. We use the units in which $G = c = 1$ and the signature convention $(-+++)$.

II. BASIC EQUATIONS

A. $3+1$ formalism

We here present the $3+1$ formalism of the Einstein equations according to Nakamura *et al.* [30]. The line element in four-dimensional spacetimes is written in the following form,

$$ds^2 = -\alpha^2 dt^2 + \gamma_{ij}(dx^i + \beta^i dt)(dx^j + \beta^j dt), \quad (2.1)$$

where α, β^i and γ_{ij} are the lapse function, shift vector and spatial metric, respectively. The Latin uppercase indices run over 1 to 3 and we drop and raise them by γ_{ij} and its inverse γ^{ij}, respectively, unless otherwise specified. The spacetime metric $g_{\mu\nu}$ and its inverse $g^{\mu\nu}$ are given by

$$g_{\mu\nu} = \begin{pmatrix} -\alpha^2 + \beta_i\beta^i & \beta_i \\ \beta_j & \gamma_{ij} \end{pmatrix} \quad \text{and}$$

$$g^{\mu\nu} = \begin{pmatrix} -\frac{1}{\alpha^2} & \frac{\beta^i}{\alpha^2} \\ \frac{\beta^j}{\alpha^2} & \gamma^{ij} - \frac{\beta^i\beta^j}{\alpha^2} \end{pmatrix}, \quad (2.2)$$

respectively, where the Greek indices run over 0 to 3. Because of the construction of the inverse matrix, we find $g = -\alpha^2\gamma$, where $g = \det(g_{\mu\nu})$ and $\gamma = \det(\gamma_{ij})$. The covariant

and contravariant components of the normal unit vector to the $t = $ const hypersurface Σ are given by

$$n_\mu = (-\alpha, 0, 0, 0) \quad \text{and} \quad n^\mu = \left(\frac{1}{\alpha}, -\frac{\beta^i}{\alpha}\right), \qquad (2.3)$$

respectively. The projection tensor to Σ is defined as $h_{\mu\nu} := g_{\mu\nu} + n_\mu n_\nu$.

The stress-energy tensor for the matter fields $T_{\mu\nu}$ is decomposed into the following form,

$$T_{\mu\nu} = E n_\mu n_\nu + J_\mu n_\nu + J_\nu n_\mu + S_{\alpha\beta} h_\mu^\alpha h_\nu^\beta, \qquad (2.4)$$

where $E := T_{\mu\nu} n^\mu n^\nu$, $J_\alpha := -T_{\mu\nu} h_\alpha^\mu n^\nu$ and $S_{\alpha\beta} := T_{\mu\nu} h_\alpha^\mu h_\beta^\nu$.

The Einstein equation $G_{\mu\nu} = 8\pi T_{\mu\nu}$ can be written in the following set of equations. The Hamiltonian constraint $G^{\mu\nu} n_\mu n_\nu = 8\pi T^{\mu\nu} n_\mu n_\nu$ and momentum constraint $G^{\mu\nu} n_\mu h_{\nu i} = 8\pi T^{\mu\nu} n_\mu h_{\nu i}$ reduce to

$$\mathcal{R} + K^2 - K_{ij} K^{ij} = 16\pi E \qquad (2.5)$$

and

$$\mathcal{D}_j K_i^j - \mathcal{D}_i K = 8\pi J_i, \qquad (2.6)$$

respectively, where $\mathcal{D}_i$ and $\mathcal{R}$ denote the covariant derivative and Ricci scalar with respect to γ_{ij}, respectively, K_{ij} is the extrinsic curvature of Σ defined by

$$K_{ij} := -h_i^\mu h_j^\nu n_{\mu;\nu} = -\frac{1}{2\alpha}(\gamma_{ij,t} - \mathcal{D}_j \beta_i - \mathcal{D}_i \beta_j), \qquad (2.7)$$

and $K := \gamma^{ij} K_{ij}$. Note that the semicolon denotes the covariant derivative with respect to $g_{\mu\nu}$.

The evolution equations $G^{\mu\nu} h_{\mu i} h_{\nu j} = 8\pi T^{\mu\nu} h_{\mu i} h_{\nu j}$ are given by

$$K_{ij,t} = \alpha(\mathcal{R}_{ij} + K K_{ij}) - 2\alpha K_{il} K_j^l$$
$$- 8\pi\alpha\left[S_{ij} + \frac{1}{2}\gamma_{ij}(E - S_l^l)\right] - \mathcal{D}_j \mathcal{D}_i \alpha + (\mathcal{D}_j \beta^m) K_{mi}$$
$$+ (\mathcal{D}_i \beta^m) K_{mj} + \beta^m \mathcal{D}_m K_{ij}, \qquad (2.8)$$

where $\mathcal{R}_{ij}$ is the Ricci tensor with respect to γ_{ij} on Σ with $\mathcal{R} = \gamma^{ij} \mathcal{R}_{ij}$. Equation (2.7) can be rewritten in the following form:

$$\gamma_{ij,t} = -2\alpha K_{ij} + \mathcal{D}_j \beta_i + \mathcal{D}_i \beta_j. \qquad (2.9)$$

The conservation law $T^{\mu\nu}{}_{;\nu} = 0$ is decomposed into $T^{\mu\nu}{}_{;\nu} n_\mu = 0$ and $T^{\mu\nu}{}_{;\nu} h_{\mu m} = 0$. Assuming a perfect fluid,

$$T_{\mu\nu} = (\rho + p) u_\mu u_\nu + p g_{\mu\nu}, \qquad (2.10)$$

where u^μ is the four-velocity of the fluid element which is normalized as $u^\mu u_\mu = -1$, they reduce to

$$(\sqrt{\gamma} E)_{,t} + (\sqrt{\gamma} E v^l)_{,l}$$
$$= -[\sqrt{\gamma} p(v^l + \beta^l)]_{,l} + \alpha\sqrt{\gamma} p K - \alpha_{,l}\sqrt{\gamma} J^l$$
$$+ \frac{\alpha\sqrt{\gamma} J^l J^m K_{lm}}{E + p} \qquad (2.11)$$

and

$$(\sqrt{\gamma} J_m)_{,t} + (\sqrt{\gamma} J_m v^l)_{,l} = -\alpha\sqrt{\gamma} p_{,m} - \sqrt{\gamma}(p + E)\alpha_{,m}$$
$$+ \frac{\alpha\sqrt{\gamma}\gamma_{kl,m} J^k J^l}{2(p + E)} + \sqrt{\gamma} J_l \beta^l_{,m}, \qquad (2.12)$$

respectively, where

$$v^l := \frac{u^l}{u^t} \qquad (2.13)$$

is the coordinate three-velocity of the fluid element. It is often useful to define the "baryon" or conserved number density n and the conservation law $(nu^\mu)_{;\mu} = 0$ gives

$$(\sqrt{\gamma}\alpha u^t n)_{,t} + (\sqrt{\gamma}\alpha u^t n v^l)_{,l} = 0. \qquad (2.14)$$

The energy conservation gives

$$\frac{dn}{n} = \frac{d\rho}{\rho + p}. \qquad (2.15)$$

The expressions for the four-velocity of the fluid element are rather complicated. In fact, Eq. (2.13) implies (Lyth et al. [22])

$$u^t = \frac{1}{\sqrt{\alpha^2 - (\beta_k + v_k)(\beta^k + v^k)}}, \qquad (2.16)$$

$$u^i = u^t v^i, \qquad (2.17)$$

$$u_t = -u^t[\alpha^2 - \beta^k(\beta_k + v_k)], \qquad (2.18)$$

$$u_i = u^t(v_i + \beta_i), \qquad (2.19)$$

where $v_i = \gamma_{ij} v^j$. We can write down E, J_i and S_{ij} as

$$E = (\rho + p)w^2 - p, \qquad (2.20)$$

$$J_i = \frac{w^2}{\alpha}(\rho + p)(v_i + \beta_i), \qquad (2.21)$$

and

$$S_{ij} = p\gamma_{ij} + \frac{J_i J_j}{E + p}, \qquad (2.22)$$

respectively, where

$$w := \alpha u^t = [1 - \alpha^{-2}(\beta_k + v_k)(\beta^k + v^k)]^{-1/2}. \quad (2.23)$$

B. Cosmological conformal decomposition

Here we briefly revisit the cosmological conformal decomposition according to Shibata and Sasaki [9]. See also Gourgoulhon [31]. We decompose the spatial metric γ_{ij} into the following form:

$$\gamma_{ij} = \psi^4 a^2(t)\tilde{\gamma}_{ij}. \quad (2.24)$$

We choose $\tilde{\gamma}_{ij}$ so that $\tilde{\gamma} = \det(\tilde{\gamma}_{ij})$ is time-independent and equal to $\eta = \det(\eta_{ij})$, where η_{ij} is a time-independent metric of the flat three-space. The function $a(t)$ is the scale factor of the reference universe. The extrinsic curvature is decomposed as

$$K_{ij} = A_{ij} + \frac{\gamma_{ij}}{3}K, \quad (2.25)$$

where A_{ij} is traceless by definition. We also define $\tilde{A}_{ij}$ as follows:

$$A^{ij} = \psi^{-4}a^{-2}\tilde{A}^{ij} \quad \text{or} \quad A_{ij} = \psi^4 a^2\tilde{A}_{ij}. \quad (2.26)$$

Thus, $\tilde{\gamma}^{ij}\tilde{A}_{ij} = 0$ by definition. We raise and drop the Latin lowercase indices $i, j, k, \ldots$ of tilded quantities by $\tilde{\gamma}^{ij}$ and $\tilde{\gamma}_{ij}$, respectively. We define $\bar{\mathcal{D}}_i$ and $\tilde{\mathcal{D}}_i$ as the covariant derivatives with respect to η_{ij} and $\tilde{\gamma}_{ij}$, respectively. We denote the Laplacians with respect to η_{ij} and $\tilde{\gamma}_{ij}$ as $\bar{\Delta} := \eta^{ij}\bar{\mathcal{D}}_i\bar{\mathcal{D}}_j$ and $\tilde{\Delta} := \tilde{\gamma}^{ij}\tilde{\mathcal{D}}_i\tilde{\mathcal{D}}_j$, respectively.

Using this decomposition, we can rewrite $\mathcal{R}_{ij}$ as follows,

$$\mathcal{R}_{ij} = \tilde{\mathcal{R}}_{ij} + \mathcal{R}^\psi_{ij}, \quad (2.27)$$

where

$$\mathcal{R}^\psi_{ij} := -\frac{2}{\psi}\tilde{\mathcal{D}}_i\tilde{\mathcal{D}}_j\psi - \frac{2}{\psi}\tilde{\gamma}_{ij}\tilde{\Delta}\psi + \frac{6}{\psi^2}\tilde{\mathcal{D}}_i\psi\tilde{\mathcal{D}}_j\psi - \frac{2}{\psi^2}\tilde{\gamma}_{ij}\tilde{\mathcal{D}}_k\psi\tilde{\mathcal{D}}^k\psi, \quad (2.28)$$

$$\tilde{\mathcal{R}}_{ij} := \frac{1}{2}[-\bar{\Delta}\tilde{\gamma}_{ij} + \bar{\mathcal{D}}_j\bar{\mathcal{D}}^k\tilde{\gamma}_{ki} + \bar{\mathcal{D}}_i\bar{\mathcal{D}}^k\tilde{\gamma}_{kj} + 2\bar{\mathcal{D}}_k(f^{kl}C_{lij}) - 2C^l{}_{kj}C^k{}_{il}], \quad (2.29)$$

$$f^{kl} := \tilde{\gamma}^{kl} - \eta^{kl}, \quad (2.30)$$

$$C^k{}_{ij} := \frac{1}{2}\tilde{\gamma}^{kl}(\bar{\mathcal{D}}_i\tilde{\gamma}_{jl} + \bar{\mathcal{D}}_j\tilde{\gamma}_{il} - \bar{\mathcal{D}}_l\tilde{\gamma}_{ij}). \quad (2.31)$$

To derive Eq. (2.29), we have used the relation

$$\tilde{\gamma}^{ij}\bar{\mathcal{D}}_k\tilde{\gamma}_{ij} = \frac{1}{\tilde{\gamma}}\bar{\mathcal{D}}_k\tilde{\gamma} = \frac{1}{\eta}\bar{\mathcal{D}}_k\eta = \eta^{ij}\bar{\mathcal{D}}_k\eta_{ij} = 0. \quad (2.32)$$

The following relations will be useful:

$$\mathcal{R}^\psi := \gamma^{ij}\mathcal{R}^\psi_{ij} = -\frac{8}{\psi^5 a^2}\tilde{\Delta}\psi, \quad (2.33)$$

$$\mathcal{R}^\psi_{ij} - \frac{1}{3}\gamma_{ij}\mathcal{R}^\psi = -\frac{2}{\psi}\left[\tilde{\mathcal{D}}_i\tilde{\mathcal{D}}_j\psi - \frac{1}{3}\tilde{\gamma}_{ij}\tilde{\Delta}\psi\right] + \frac{6}{\psi^2}\left[\tilde{\mathcal{D}}_i\psi\tilde{\mathcal{D}}_j\psi - \frac{1}{3}\tilde{\gamma}_{ij}\tilde{\mathcal{D}}^k\psi\bar{\mathcal{D}}_k\psi\right]. \quad (2.34)$$

The Hamiltonian and momentum constraints are given by

$$\mathcal{R}^k_k - \tilde{A}_{ij}\tilde{A}^{ij} + \frac{2}{3}K^2 = 16\pi E, \quad (2.35)$$

and

$$\mathcal{D}_j\tilde{A}^j_i - \frac{2}{3}\mathcal{D}_iK = 8\pi J_i, \quad (2.36)$$

respectively. These can be transformed to the following form:

$$\tilde{\Delta}\psi = \frac{\tilde{\mathcal{R}}^k_k}{8}\psi - 2\pi\psi^5 a^2 E - \frac{\psi^5 a^2}{8}\left(\tilde{A}_{ij}\tilde{A}^{ij} - \frac{2}{3}K^2\right), \quad (2.37)$$

$$\tilde{\mathcal{D}}^j(\psi^6\tilde{A}_{ij}) - \frac{2}{3}\psi^6\tilde{\mathcal{D}}_iK = 8\pi J_i\psi^6. \quad (2.38)$$

The evolution equations become

$$(\partial_t - \mathcal{L}_\beta)\tilde{A}_{ij} = \frac{1}{a^2\psi^4}\left[\alpha\left(\mathcal{R}_{ij} - \frac{\gamma_{ij}}{3}\mathcal{R}\right) - \left(D_iD_j\alpha - \frac{\gamma_{ij}}{3}D_kD^k\alpha\right)\right]$$
$$+ \alpha(K\tilde{A}_{ij} - 2\tilde{A}_{ik}\tilde{A}_j^k) - \frac{2}{3}(\bar{\mathcal{D}}_k\beta^k)\tilde{A}_{ij} - \frac{8\pi\alpha}{a^2\psi^4}\left(S_{ij} - \frac{\gamma_{ij}}{3}S_k^k\right), \tag{2.39}$$

$$(\partial_t - \mathcal{L}_\beta)\psi = -\frac{\dot{a}}{2a}\psi + \frac{\psi}{6}(-\alpha K + \bar{\mathcal{D}}_k\beta^k), \tag{2.40}$$

$$(\partial_t - \mathcal{L}_\beta)K = \alpha\left(\tilde{A}_{ij}\tilde{A}^{ij} + \frac{1}{3}K^2\right) - D_kD^k\alpha + 4\pi\alpha(E + S_k^k), \tag{2.41}$$

where $\mathcal{L}_\beta$ is the Lie derivative along β^i and acts on a scalar field f and a tensor field f_{ij} as follows:

$$\mathcal{L}_\beta f = \beta^k f_{,k}, \tag{2.42}$$

$$\mathcal{L}_\beta f_{ij} = \beta^k f_{ij,k} + \beta_{,i}^k f_{kj} + \beta_{,j}^k f_{ki}. \tag{2.43}$$

The definition of the extrinsic curvature yields

$$(\partial_t - \mathcal{L}_\beta)\tilde{\gamma}_{ij} = -2\alpha\tilde{A}_{ij} - \frac{2}{3}\tilde{\gamma}_{ij}\bar{\mathcal{D}}_k\beta^k. \tag{2.44}$$

The hydrodynamical equations (2.11), (2.12) and (2.14) are, respectively, written in the form

$$[\psi^6a^3\{(\rho+p)w^2 - p\}]_{,t} + \frac{1}{\sqrt{\eta}}[\sqrt{\eta}\psi^6a^3\{(\rho+p)w^2 - p\}v^l]_{,l}$$
$$= -\frac{1}{\sqrt{\eta}}[\sqrt{\eta}\psi^6a^3p(v^l+\beta^l)]_{,l} + \alpha\psi^6a^3pK - \alpha^{-1}\alpha_{,l}\psi^6a^3w^2(\rho+p)(v^l+\beta^l)$$
$$+ \alpha^{-1}\psi^{10}a^5w^2(\rho+p)(v^l+\beta^l)(v^m+\beta^m)\left(\tilde{A}_{lm} + \frac{\tilde{\gamma}_{lm}}{3}K\right), \tag{2.45}$$

A. Basic assumptions

To be precise, we focus on some fixed time and put a fictitious parameter ϵ in front of the spatial partial derivative, e.g., $\partial_i \to \epsilon\partial_i$. We expand exact solutions in a power series of ϵ, require the field equations at each order and finally set $\epsilon = 1$. This scheme is called the gradient expansion. We assume that the spacetime is approximately smooth for scales greater than k^{-1} in terms of the comoving coordinate. This implies that the physical scale of smoothing is $L = a/k$. Since the Hubble length H_b^{-1} is the only natural scale of the cosmological evolution, we can make the identification $\epsilon = H_b^{-1}/L = k/(aH_b)$. Thus, the gradient expansion implies that we assume that the smoothing length L is much larger than the Hubble length, i.e., $L \gg H_b^{-1}$.

Based on the above consideration, we make two key assumptions. First, we assume that ψ is identically unity somewhere in the universe. This makes $a(t)$ be the scale factor for that part of the universe. Second, we assume that in the limit $\epsilon \to 0$, the universe becomes locally homogeneous and isotropic, i.e., an FRW universe, which we additionally assume is flat. Thus, the measurable parts of the metric should reduce to the flat FRW one in the

$$(w\psi^6a^3(\rho+p)u_j)_{,t} + \frac{1}{\sqrt{\eta}}(\sqrt{\eta}w\psi^6a^3(\rho+p)v^ku_j)_{,k}$$
$$= -\alpha\psi^6a^3p_{,j} + w\psi^6a^3(\rho+p)\left(-w\alpha_{,j} + u_k\beta_{,j}^k - \frac{u_ku_l}{2u^t}\gamma_{,j}^{kl}\right), \tag{2.46}$$

and

$$(w\psi^6a^3n)_{,t} + \frac{1}{\sqrt{\eta}}(\sqrt{\eta}w\psi^6a^3nv^k)_{,k} = 0. \tag{2.47}$$

We can define the background Hubble parameter H_b as $H_b := \dot{a}/a$. The scale factor $a(t)$ will be that of the flat FRW universe in the next section, although the field equations up to here are independent from this choice.

III. LONG-WAVELENGTH SCHEME

We here review the long-wavelength scheme based on Lyth *et al.* [22].

smoothing scale L which is much larger than the Hubble length H_b^{-1}. This means that there exists a coordinate system with which the metric of any local region is written in the following form:

$$ds^2 = -dt^2 + a^2 \eta_{ij} dx^i dx^j. \tag{3.1}$$

Hence, we assume $\beta^i = O(\epsilon)$, although this is a matter of coordinate choice. As for the spatial metric, a homogeneous time-independent $\tilde{\gamma}_{ij}$ can be transformed away, while a homogeneous time-dependent $\tilde{\gamma}_{ij}$ should not exist by the present assumption. Since the term of $O(\epsilon)$ in $\dot{\tilde{\gamma}}_{ij}$ turns out to be decaying, we assume $\dot{\tilde{\gamma}}_{ij} = O(\epsilon^2)$. The above assumptions are partially justified in the literature in the context of inflationary cosmology [32,33].

B. Energy conservation and curvature perturbation

Let us consider a perfect fluid given by Eq. (2.10) and choose the spatial coordinates so that the worldlines on which $x^i = $ const coincide with the worldlines of the fluid elements, which is called the comoving threading. This implies $v^i = u^i/u^t = 0$. Then, u^μ is given by

$$u^\mu = \left(\frac{1}{\sqrt{\alpha^2 - \beta_k \beta^k}}, 0, 0, 0 \right) = \left(\frac{1}{\alpha}, 0, 0, 0 \right) + O(\epsilon^2), \tag{3.2}$$

$$u_\mu = \left(-\sqrt{\alpha^2 - \beta^k \beta_k}, \frac{\beta_i}{\sqrt{\alpha^2 - \beta^k \beta_k}} \right) = \left(-\alpha, \frac{\beta_i}{\alpha} \right) + O(\epsilon^2). \tag{3.3}$$

The expansion of u^μ is given by

$$\theta := u^\mu_{;\mu} = \frac{1}{\alpha \psi^6 a^3} \partial_t \left(\frac{\alpha \psi^6 a^3}{\sqrt{\alpha^2 - \beta^i \beta_i}} \right) = \frac{3}{\alpha} \frac{(\psi^2 a)_{,t}}{\psi^2 a} + O(\epsilon^2), \tag{3.4}$$

where it should be noted that $\tilde{\gamma}$ is time independent. The relation between t and the proper time τ along the worldlines of the fluid elements is given by

$$\frac{dt}{d\tau} = u^t = \frac{1}{\sqrt{\alpha^2 - \beta^i \beta_i}}. \tag{3.5}$$

The energy conservation law

$$0 = -u_\mu T^{\mu\nu}_{;\nu} = \frac{d\rho}{d\tau} + (\rho + p)\theta \tag{3.6}$$

implies

$$\frac{\dot{a}}{a} + 2\frac{\dot{\psi}}{\psi} = -\frac{1}{3}\frac{\dot{\rho}}{\rho + p} + O(\epsilon^2). \tag{3.7}$$

If we choose the *uniform-density slicing*, on which $\rho = $ const, and assume that the pressure is homogeneous to $O(\epsilon)$, $\dot{\psi}/\psi$ is also homogeneous to $O(\epsilon)$. Since we assume that ψ is identically unity at some point, we can conclude that ψ is time independent to $O(\epsilon)$, i.e.,

$$\dot{\psi} = O(\epsilon^2). \tag{3.8}$$

The expansion of n^μ is given by

$$\theta_n := n^\mu_{;\mu} = \frac{3}{\alpha} \frac{(\psi^2 a)_{,t}}{\psi^2 a} - \frac{1}{\alpha \psi^6 a^3 \sqrt{\eta}} \partial_i (\sqrt{\eta} \psi^6 a^3 \beta^i), \tag{3.9}$$

and this is related to the trace of the extrinsic curvature through

$$\theta_n = -K. \tag{3.10}$$

Since $\beta^i = O(\epsilon)$, Eqs. (3.4) and (3.9) imply

$$\theta = \theta_n + O(\epsilon^2). \tag{3.11}$$

This shows the equivalence between θ and θ_n to $O(\epsilon)$. For convenience, we introduce the Hubble parameter $\tilde{H}$ as

$$\tilde{H} := \frac{1}{3}\theta_n = \frac{1}{\alpha} \frac{(\psi^2 a)_{,t}}{\psi^2 a} + O(\epsilon^2). \tag{3.12}$$

From Eqs. (3.4), (3.6), (3.11) and (3.12), we find

$$\frac{d\rho}{d\tau} = -3\tilde{H}(\rho + p) + O(\epsilon^2). \tag{3.13}$$

C. Equivalence among different time slicings

We use the following terminology about the slicing conditions. We call the slicing which is orthogonal to the fluid worldlines, namely, $n^\mu = u^\mu$, the *comoving slicing*. This is independent of the comoving threading with which the worldline of the fluid coincides with that of the constant spatial coordinates. We call the slicing on which the trace of the extrinsic curvature is uniform the *constant mean curvature* (CMC) *slicing*. Although this is sometimes called the uniform-Hubble slicing, we here avoid this terminology because of the ambiguity in the definition of the Hubble parameter in inhomogeneous cosmology. We call the slicing with $\alpha = 1$ the *geodesic slicing*.

The comoving slicing implies $u_i = 0$ and, hence, $J_i = 0$. This is possible only if u^μ is vorticity free because of the Frobenius theorem. This condition is physically reasonable in the early universe because the vorticity is not generated from vacuum fluctuation during inflation and because the vorticity is conserved for a perfect fluid in any spacetime.

Therefore, in the comoving slicing, the momentum constraint (2.36) implies

$$\partial_i \tilde{H} = O(\epsilon^3), \qquad (3.14)$$

and the Hamiltonian constraint (2.35) gives

$$\tilde{H}^2 = \frac{8\pi}{3}\rho + O(\epsilon^2), \qquad (3.15)$$

implying

$$\partial_i \rho = O(\epsilon^3). \qquad (3.16)$$

That is $\delta\rho = O(\epsilon^2)$ and $\delta\tilde{H} = O(\epsilon^2)$ in the comoving slicing, where $\delta\rho$ and $\delta\tilde{H}$ are the inhomogeneous parts of ρ and $\tilde{H}$, respectively. This means that the uniform-density, CMC and comoving slicings coincide to $O(\epsilon)$. This also guarantees that ψ is time independent to $O(\epsilon)$ in each of those slicings and the time-dependent part appears only from $O(\epsilon^2)$.

From Eq. (3.13), we find

$$\frac{1}{\alpha}\dot{\rho} = -3\tilde{H}(\rho + p) + O(\epsilon^2). \qquad (3.17)$$

Since ρ is homogeneous to $O(\epsilon)$, $\dot{\rho}$ is also homogeneous to $O(\epsilon)$. Hence, the lapse function is given by

$$\alpha = \frac{A(t)}{\rho + p} + O(\epsilon^2), \qquad (3.18)$$

where $A(t)$ is a function of t. If p is homogeneous to $O(\epsilon)$, which is the case for the barotropic equation of state, α is also homogeneous to $O(\epsilon)$ and we can choose $\alpha = 1$ by rescaling the time coordinate. Thus, the geodesic slicing is also equivalent to the uniform-density slicing to $O(\epsilon)$.

IV. LONG-WAVELENGTH SOLUTIONS

A. Gradient expansion

Here we derive the expansion of the physical quantities based on the assumption of $\beta^i = O(\epsilon)$ and $\dot{\tilde{\gamma}}_{ij} = O(\epsilon^2)$. In the limit $\epsilon \to 0$, the metric functions α and ψ are assumed to be locally homogeneous. We can use the scaling of time so that $\alpha = 1$ locally in this limit and this suits the metric form given by Eq. (3.1).

From Eq. (2.44), we find $\tilde{A}_{ij} = O(\epsilon^2)$. We are still allowed to take general time slicings on which the density is uniform to $O(\epsilon)$. As inhomogeneity appears in the mean curvature $K = -\theta_n$ from $O(\epsilon^2)$, $J_i = O(\epsilon^3)$ follows from Eq. (2.38). Combining this with Eq. (2.21), we find $v_i + \beta_i = O(\epsilon^3)$. Therefore, since $\beta^i = O(\epsilon)$, we find $v^i = O(\epsilon)$. Since $\dot{\tilde{\gamma}}_{ij} = O(\epsilon^2)$, we can assign $h_{ij} = O(\epsilon^2)$

using an appropriate coordinate transformation, where $h_{ij} := \tilde{\gamma}_{ij} - \eta_{ij}$.

In summary, if we assume

$$\beta^i = O(\epsilon), \qquad \dot{\tilde{\gamma}}_{ij} = O(\epsilon^2), \qquad (4.1)$$

then we deduce

$$\psi = \psi(x^k) = O(\epsilon^0), \qquad v^i = O(\epsilon), \qquad \delta = O(\epsilon^2),$$
$$\tilde{A}_{ij} = O(\epsilon^2), \qquad h_{ij} = O(\epsilon^2), \qquad \chi = O(\epsilon^2),$$
$$\kappa = O(\epsilon^2), \qquad (4.2)$$

where

$$\delta := \frac{\rho - \rho_b}{\rho_b}, \qquad h_{ij} := \tilde{\gamma}_{ij} - \eta_{ij}, \qquad \chi := \alpha - 1,$$
$$\kappa := \frac{K - K_b}{K_b}. \qquad (4.3)$$

For later convenience, we define

$$\delta_n := \frac{n - n_b}{n_b} = \frac{1}{1 + R}\delta + O(\epsilon^4),$$
$$\delta_p := \frac{p - p_b}{p_b} = \frac{c_s^2}{R}\delta + O(\epsilon^4), \qquad (4.4)$$

where we have used Eq. (2.15) and defined

$$R := \frac{p_b}{\rho_b}, \qquad c_s^2 := \left(\frac{dp}{d\rho}\right)_b. \qquad (4.5)$$

Equations (2.11), (2.37), (2.40), (2.41) and (2.47) in $O(\epsilon^0)$ give

$$K_b = -3\frac{\dot{a}}{a}, \qquad (4.6)$$

$$\left(\frac{\dot{a}}{a}\right)^2 = \frac{8\pi}{3}\rho_b, \qquad (4.7)$$

$$\frac{\ddot{a}}{a} = -\frac{4\pi}{3}(\rho_b + 3p_b), \qquad (4.8)$$

$$\dot{\rho}_b = -3(\rho_b + p_b)\frac{\dot{a}}{a}, \qquad (4.9)$$

$$(a^3 n_b)_{,t} = 0. \qquad (4.10)$$

This is a complete set of the Friedmann equations with spatially flat geometry.

To discuss the next order term in ψ, we decompose it into the following form,

$$\psi(t, x^k) = \Psi(x^k)(1 + \xi(t, x^k)), \qquad (4.11)$$

where $\Psi = O(\epsilon^0)$ and $\xi = O(\epsilon^2)$. It is also useful to note $w = 1 + O(\epsilon^6)$ from Eq. (2.23).

B. Field equations in general gauge

As we have seen in the previous section, the comoving, CMC, uniform-density and geodesic slicings coincide to $O(\epsilon)$. This ensures that we can consistently apply the gradient expansion in any of these four slicings. Here we derive the field equations in general gauge which is consistent with the long-wavelength scheme by generalizing the formulation by Shibata and Sasaki [9].

First, Eq. (2.40) results in $\dot{\Psi} = 0$. This is the starting point of the formulation. Then, Eqs. (2.45) and (2.47) yield

$$\dot{\delta} + 6\dot{\xi} + \nabla_k v^k - 3H_bR(\delta - \delta_p - \chi - \kappa) = O(\epsilon^4), \quad (4.12)$$

and

$$\dot{\delta}_n + 6\dot{\xi} + \nabla_k v^k = O(\epsilon^4), \quad (4.13)$$

respectively, where

$$\nabla_k v^k := \frac{1}{\Psi^6 \eta^{1/2}} \partial_k(\eta^{1/2} \Psi^6 v^k). \quad (4.14)$$

Equations (2.46), (2.40), (2.37), (2.41), (2.44), (2.39), (2.38) yield

$$\partial_t[a^3(1 + R)\rho_b u_j] = -a^3 \rho_b[R\partial_j\delta_p + (1 + R)\partial_j\chi] + O(\epsilon^5), \quad (4.15)$$

$$6\dot{\xi} - 3H_b(\chi + \kappa) - \nabla_k\beta^k = O(\epsilon^4), \quad (4.16)$$

$$\bar{\Delta}\Psi = -2\pi\Psi^5 a^2\rho_b(\delta - 2\kappa) + O(\epsilon^4), \quad (4.17)$$

$$H_b^{-1}\dot{\kappa} = \frac{1}{2}(3R - 1)\kappa - \frac{3}{2}(1 + R)\chi - \frac{1}{2}(\delta + 3R\delta_p) + O(\epsilon^4), \quad (4.18)$$

$$\partial_t h_{ij} = -2\tilde{A}_{ij} + \eta_{ik}\bar{D}_j\beta^k + \eta_{jk}\bar{D}_i\beta^k - \frac{2}{3}\eta_{ij}\bar{D}_k\beta^k + O(\epsilon^4), \quad (4.19)$$

$$\partial_t\tilde{A}_{ij} + \frac{3\dot{a}}{a}\tilde{A}_{ij} = \frac{1}{a^2\Psi^4}\left[-\frac{2}{\Psi}\left(\bar{D}_i\bar{D}_j\Psi - \frac{1}{3}\eta_{ij}\bar{\Delta}\Psi\right) + \frac{6}{\Psi^2}\left(\bar{D}_i\Psi\bar{D}_j\Psi - \frac{1}{3}\eta_{ij}\bar{D}^k\Psi\bar{D}_k\Psi\right)\right] + O(\epsilon^4), \quad (4.20)$$

$$\bar{D}_i(\Psi^6\tilde{A}_j^i) + 2H_b\Psi^6\bar{D}_j\kappa = 8\pi\Psi^6(1 + R)\rho_b u_j + O(\epsilon^5), \quad (4.21)$$

respectively, where we have used

$$E + S_k^k = \rho + 3p + O(\epsilon^6), \quad (4.22)$$

$$S_{ij} - \frac{\gamma_{ij}}{3}S_k^k = O(\epsilon^6), \quad (4.23)$$

following from Eqs. (2.20)–(2.22). Equations (4.12), (4.13) and (4.16) give

$$\dot{\delta} - \dot{\delta}_n - 3H_bR(\delta - \delta_p - \chi - \kappa) = O(\epsilon^4), \quad (4.24)$$

$$\dot{\delta} - 3H_bR(\delta - \delta_p) + 3(1 + R)H_b(\chi + \kappa) = O(\epsilon^4), \quad (4.25)$$

$$\dot{\delta} - (1 + R)\dot{\delta}_n - 3H_bR(\delta - \delta_p) = O(\epsilon^4), \quad (4.26)$$

where it should be noted that $\nabla_k(\beta^k + v^k) = O(\epsilon^4)$.

C. Long-wavelength solutions

1. $\tilde{A}_{ij}$ and h_{ij}

We can see that $\tilde{A}_{ij}$ and h_{ij} are not sensitive to the choice of time slicings to $O(\epsilon^2)$. Equation (4.20) admits the following solution for $\tilde{A}_{ij}$,

$$\tilde{A}_{ij} = p_{ij}\frac{1}{a^3}\left[\int_0^a \frac{d\tilde{a}}{H_b(\tilde{a})}\right] + O(\epsilon^4), \quad (4.27)$$

where we have put

$$p_{ij}(x^k) := \frac{1}{\Psi^4}\left[-\frac{2}{\Psi}\left(\bar{D}_i\bar{D}_j\Psi - \frac{1}{3}\eta_{ij}\bar{\Delta}\Psi\right) + \frac{6}{\Psi^2}\left(\bar{D}_i\Psi\bar{D}_j\Psi - \frac{1}{3}\eta_{ij}\bar{D}^k\Psi\bar{D}_k\Psi\right)\right], \quad (4.28)$$

and we have omitted the integration constant because it generally gives a decaying mode.

The expression of h_{ij} depends on the choice of the spatial coordinates. For the normal coordinates, where $\beta^i = 0$, by integrating Eq. (4.19), we find

$$h_{ij} = -2p_{ij}\int_0^a \frac{d\tilde{a}}{\tilde{a}^4 H_b(\tilde{a})}\int_0^{\tilde{a}} \frac{d\bar{a}}{H_b(\bar{a})} + C_{ij} + O(\epsilon^4). \quad (4.29)$$

We drop the constant tensor C_{ij} so that $h_{ij} \to 0$ in the limit $t \to 0$ by choosing appropriate spatial coordinates. Of course, other coordinate conditions may be useful. For example, in spherical symmetry, we can even have $h_{ij} = 0$ identically, for which β^i is accordingly determined. This is called the conformally flat spatial coordinates.

If we assume $\Gamma = \text{const}$, we have the background solution from Eq. (4.7) as

$$a = a_0 \left(\frac{t}{t_0}\right)^{\frac{2}{3\Gamma}}, \tag{4.30}$$

and we can explicitly write $\tilde{A}_{ij}$ and h_{ij} in the following form,

$$\tilde{A}_{ij} = \frac{2}{3\Gamma + 2} p_{ij} H_b \left(\frac{1}{aH_b}\right)^2 + O(\epsilon^4), \tag{4.31}$$

$$h_{ij} = -\frac{4}{(3\Gamma + 2)(3\Gamma - 2)} p_{ij} \left(\frac{1}{aH_b}\right)^2 + O(\epsilon^4), \tag{4.32}$$

where the bottom one is obtained in the normal coordinates. $\tilde{A}_{ij}$ and h_{ij} depend on time as

$$\tilde{A}_{ij} \propto t^{1-\frac{4}{3\Gamma}} \quad \text{and} \quad h_{ij} \propto t^{2-\frac{4}{3\Gamma}}, \tag{4.33}$$

respectively.

2. CMC slicing

Hereafter, we assume $\Gamma = \text{const}$ for simplicity. Then, Eqs. (4.4) and (4.5), respectively, yield

$$\delta_n = \frac{1}{\Gamma}\delta + O(\epsilon^4), \tag{4.34}$$

$$\delta_p = \delta + O(\epsilon^4). \tag{4.35}$$

We present the solutions in the CMC slicing, where $\kappa = 0$. Equation (4.17) is solved for δ to give

$$\delta = -\frac{\bar{\Delta}\Psi}{2\pi\Psi^5 a^2 \rho_b} + O(\epsilon^4). \tag{4.36}$$

Defining

$$f(x^k) := -\frac{4}{3}\frac{\bar{\Delta}\Psi}{\Psi^5} \tag{4.37}$$

and using Eqs. (4.7) and (4.18), we can express δ and χ as follows:

$$\delta = f\left(\frac{1}{aH_b}\right)^2 + O(\epsilon^4), \tag{4.38}$$

$$\chi = -\frac{3\Gamma - 2}{3\Gamma} f\left(\frac{1}{aH_b}\right)^2 + O(\epsilon^4). \tag{4.39}$$

Then, from Eq. (4.15), we find

$$u_j = \frac{1}{3\Gamma}\partial_j f \frac{1}{a}\left[\int_0^a \frac{d\tilde{a}}{H_b(\tilde{a})} + C\right]\left(\frac{1}{aH_b}\right)^2 + O(\epsilon^5), \tag{4.40}$$

where C is a constant of integration. If C is nonvanishing, there appears a decaying mode for $1 \le \Gamma < 2$. So we assume $C = 0$. Thus, we have

$$u_j = u^t(v_j + \beta_j)$$
$$= \frac{1}{3\Gamma}\partial_j f \frac{1}{a}\left[\int_0^a \frac{d\tilde{a}}{H_b(\tilde{a})}\right]\left(\frac{1}{aH_b}\right)^2 + O(\epsilon^5). \tag{4.41}$$

We can explicitly prove that the above solves the momentum constraint equation (4.21) to $O(\epsilon^3)$, using the identity

$$\bar{D}^j(\Psi^6 p_{ij}) = \Psi^6 \bar{D}_i f. \tag{4.42}$$

If we choose the normal coordinates, where $\beta^i = 0$, v_j is obtained by Eq. (4.41) as

$$v_j = \frac{1}{3\Gamma}\partial_j f \frac{1}{a}\left[\int_0^a \frac{d\tilde{a}}{H_b(\tilde{a})}\right]\left(\frac{1}{aH_b}\right)^2 + O(\epsilon^5). \tag{4.43}$$

In this case, ξ is obtained by integrating Eq. (4.16) as

$$\xi = -\frac{1}{6\Gamma}f(x^k)\left(\frac{1}{aH_b}\right)^2 + O(\epsilon^4), \tag{4.44}$$

where the integration constant is absorbed into Ψ.

Using the background solution (4.30), we find

$$\delta = f\left(\frac{1}{aH_b}\right)^2 + O(\epsilon^4), \tag{4.45}$$

$$\kappa = 0, \tag{4.46}$$

$$\chi = -\frac{3\Gamma - 2}{3\Gamma}f\left(\frac{1}{aH_b}\right)^2 + O(\epsilon^4), \tag{4.47}$$

$$u_j = u^t(v_j + \beta_j) = \frac{2}{3\Gamma(3\Gamma + 2)}\partial_j f a\left(\frac{1}{aH_b}\right)^3 + O(\epsilon^5), \tag{4.48}$$

$$v_j = \frac{2}{3\Gamma(3\Gamma + 2)}\partial_j f a\left(\frac{1}{aH_b}\right)^3 + O(\epsilon^5), \tag{4.49}$$

$$\xi = -\frac{1}{6\Gamma}f(x^k)\left(\frac{1}{aH_b}\right)^2 + O(\epsilon^4), \tag{4.50}$$

where the last two equations are obtained in the normal coordinates. The time dependence of the perturbations is summarized as follows,

$$\delta \propto t^{2-\frac{4}{3\Gamma}}, \qquad \chi \propto t^{2-\frac{4}{3\Gamma}},$$
$$u_j = u^t(v_j + \beta_j) \propto t^{3-\frac{4}{3\Gamma}}, \qquad \xi \propto t^{2-\frac{4}{3\Gamma}},$$
$$v_j \propto t^{3-\frac{4}{3\Gamma}}, \tag{4.51}$$

where the last two equations are obtained in the normal coordinates.

3. Uniform-density slicing

The uniform density slicing implies $\delta = 0$. By the assumption $\Gamma = \text{const}$, we find $\delta_n = \delta_p = 0$. From Eqs. (4.17), (4.25) and (4.15), we find

$$\kappa = -\frac{1}{2}f\left(\frac{1}{aH_b}\right)^2 + O(\epsilon^4), \tag{4.52}$$

$$\chi = \frac{1}{2}f\left(\frac{1}{aH_b}\right)^2 + O(\epsilon^4), \tag{4.53}$$

$$
\begin{aligned}
u_j &= u^t(v_j + \beta_j) \\
&= -\frac{1}{2}\partial_j f \frac{1}{a}\left[\int_0^a \frac{d\tilde{a}}{H_b(\tilde{a})}\right]\left(\frac{1}{aH_b}\right)^2 + O(\epsilon^5), \tag{4.54}
\end{aligned}
$$

where f is defined by Eq. (4.37). We can explicitly show that the momentum constraint (4.21) is satisfied to this order. Using the background solution (4.30), we have

$$\delta = 0, \tag{4.55}$$

$$\kappa = -\frac{1}{2}f\left(\frac{1}{aH_b}\right)^2 + O(\epsilon^4), \tag{4.56}$$

$$\chi = \frac{1}{2}f\left(\frac{1}{aH_b}\right)^2 + O(\epsilon^4), \tag{4.57}$$

$$v_j = -\frac{1}{3\Gamma + 2}\partial_j f a\left(\frac{1}{aH_b}\right)^3 + O(\epsilon^5), \tag{4.58}$$

$$\xi = O(\epsilon^4), \tag{4.59}$$

where the last two expressions are obtained in the normal coordinates, and in the bottom equation we have used that ξ can be shown to be time independent and is absorbed into Ψ to $O(\epsilon^2)$. Therefore, in the uniform-density slicing with the normal coordinates, ψ is time independent to $O(\epsilon^2)$.

4. Comoving slicing

In the comoving slicing, $u^\mu = n^\mu$ and hence

$$u_i = 0. \tag{4.60}$$

Then, Eq. (4.15) implies

$$(\Gamma - 1)\delta + \Gamma\chi = O(\epsilon^4). \tag{4.61}$$

Using this and Eqs. (4.18) and (4.24), we find

$$\partial_s \kappa = \frac{1}{2}(3\Gamma - 4)\kappa - \frac{1}{2}\delta + O(\epsilon^4), \tag{4.62}$$

$$\partial_s \delta = -3\Gamma\kappa + 3(\Gamma - 1)\delta + O(\epsilon^4), \tag{4.63}$$

where we put $s = \ln a$. The matrix

$$\begin{pmatrix} (3\Gamma - 4)/2 & -1/2 \\ -3\Gamma & 3(\Gamma - 1) \end{pmatrix} \tag{4.64}$$

has eigenvalues $(3\Gamma - 2)$ and $3(\Gamma - 2)/2$ with associated eigenvectors

$$\begin{pmatrix} 1 \\ -3\Gamma \end{pmatrix} \quad \text{and} \quad \begin{pmatrix} 1 \\ 2 \end{pmatrix}, \tag{4.65}$$

respectively. Therefore, the general solution for κ and δ is given by

$$\begin{pmatrix} \kappa \\ \delta \end{pmatrix} = C_1\begin{pmatrix} 1 \\ -3\Gamma \end{pmatrix}a^{3\Gamma - 2} + C_2\begin{pmatrix} 1 \\ 2 \end{pmatrix}a^{\frac{3}{2}(\Gamma - 2)} + O(\epsilon^4), \tag{4.66}$$

where C_1 and C_2 are integration constants. For $2/3 < \Gamma < 2$, the first term grows, while the second term decays in time. Hence we drop the second term by choosing $C_2 = 0$. Thus, we have

$$\kappa = -\frac{1}{3\Gamma}\delta + O(\epsilon^4). \tag{4.67}$$

Substituting this into Eq. (4.17), we have

$$\delta = \frac{3\Gamma}{3\Gamma + 2}f\left(\frac{1}{aH_b}\right)^2, \tag{4.68}$$

where f is defined by Eq. (4.37). It should be noted that the time dependence of δ is consistent with the first term on the right-hand side of Eq. (4.66). Now it is straightforward to see that κ, χ and ξ are obtained by

$$\kappa = -\frac{1}{3\Gamma + 2}f\left(\frac{1}{aH_b}\right)^2 + O(\epsilon^4), \tag{4.69}$$

$$\chi = -\frac{3(\Gamma - 1)}{3\Gamma + 2}f\left(\frac{1}{aH_b}\right)^2 + O(\epsilon^4), \tag{4.70}$$

$$u_j = 0, \tag{4.71}$$

$$v_j = 0, \tag{4.72}$$

$$\xi = -\frac{1}{2(3\Gamma + 2)}f\left(\frac{1}{aH_b}\right)^2 + O(\epsilon^4), \tag{4.73}$$

where the last two expressions are obtained in the normal coordinates. We can explicitly show that the momentum constraint (4.21) is satisfied to this order. The combination of the comoving slicing and comoving threading, i.e., $u_i = \beta_i = 0$, is called the comoving gauge.

5. Geodesic slicing

In the geodesic slicing, it is straightforward to obtain

$$\delta = \frac{3\Gamma}{9\Gamma - 4} f \left(\frac{1}{aH_b} \right)^2 + O(\epsilon^4), \qquad (4.74)$$

$$\kappa = -\frac{3\Gamma - 2}{9\Gamma - 4} f \left(\frac{1}{aH_b} \right)^2 + O(\epsilon^4), \qquad (4.75)$$

$$\chi = 0, \qquad (4.76)$$

$$u_j = -\frac{6(\Gamma - 1)}{(9\Gamma - 4)(3\Gamma + 2)} \partial_j f a \left(\frac{1}{aH_b} \right)^3 + O(\epsilon^5), \quad (4.77)$$

$$v_j = -\frac{6(\Gamma - 1)}{(9\Gamma - 4)(3\Gamma + 2)} \partial_j f a \left(\frac{1}{aH_b} \right)^3 + O(\epsilon^5), \quad (4.78)$$

$$\xi = -\frac{1}{2(9\Gamma - 4)} f \left(\frac{1}{aH_b} \right)^2 + O(\epsilon^4), \qquad (4.79)$$

where the last two expressions are obtained in the normal coordinates. The gauge condition of $\alpha = 1$ and $\beta^i = 0$, i.e., the geodesic slicing with the normal coordinates, is called the synchronous gauge.

6. Relations among the different time slicings

In Sec. III, we have seen that the slicings in the long-wavelength scheme coincide to $O(\epsilon)$. This means that the zeroth-order curvature variable $\Psi = \Psi(x^k)$ should be common, i.e.,

$$\Psi_{CMC} = \Psi_{UD} = \Psi_C = \Psi_G \qquad (4.80)$$

for the same spacetime, where CMC, UD, C and G stand for the CMC slicing, uniform-density slicing, comoving slicing, and geodesic slicing, respectively. Using the results obtained in Sec. IV C, we can find the relations among the perturbations in the different slicings. Irrespective of the choice of β^i, we can conclude

$$\tilde{A}_{ij,CMC} = \tilde{A}_{ij,UD} + O(\epsilon^4) = \tilde{A}_{ij,C} + O(\epsilon^4)$$
$$= \tilde{A}_{ij,G} + O(\epsilon^4) \qquad (4.81)$$

and

$$\delta_C = \frac{3\Gamma}{3\Gamma + 2} \delta_{CMC} + O(\epsilon^4), \qquad \delta_{UD} = 0,$$

$$\delta_G = \frac{3\Gamma}{9\Gamma - 4} \delta_{CMC}, \qquad (4.82)$$

$$\kappa_{CMC} = 0, \qquad \kappa_C = \frac{2}{3\Gamma + 2} \kappa_{UD} + O(\epsilon^4),$$

$$\kappa_G = \frac{2(3\Gamma - 2)}{9\Gamma - 4} \kappa_{UD} \qquad (4.83)$$

$$\chi_C = \frac{9\Gamma(\Gamma - 1)}{(3\Gamma - 2)(3\Gamma + 2)} \chi_{CMC} + O(\epsilon^4),$$

$$\chi_{UD} = -\frac{3\Gamma}{2(3\Gamma - 2)} \chi_{CMC} + O(\epsilon^4), \qquad \chi_G = 0, \qquad (4.84)$$

$$u_{jC} = 0, \qquad u_{jUD} = -\frac{3\Gamma}{2} u_{jCMC} + O(\epsilon^4),$$

$$u_{jG} = -\frac{9\Gamma(\Gamma - 1)}{9\Gamma - 4} u_{jCMC}. \qquad (4.85)$$

In the normal coordinates, where $\beta^i = 0$, we can also conclude the following relations:

$$h_{ij,CMC} = h_{ij,UD} + O(\epsilon^4) = h_{ij,C} + O(\epsilon^4)$$
$$= h_{ij,G} + O(\epsilon^4), \qquad (4.86)$$

$$v_{jUD} = -\frac{3\Gamma}{2} v_{jCMC} + O(\epsilon^4), \qquad v_{jC} = 0,$$

$$v_{jG} = -\frac{9\Gamma(\Gamma - 1)}{9\Gamma - 4} v_{jCMC}, \qquad (4.87)$$

$$\xi_C = \frac{3\Gamma}{3\Gamma + 2} \xi_{CMC} + O(\epsilon^4), \qquad \xi_{UD} = O(\epsilon^4),$$

$$\xi_G = \frac{3\Gamma}{9\Gamma - 4} \xi_{CMC}. \qquad (4.88)$$

V. SPHERICALLY SYMMETRIC SPACETIMES

One of the important motivations of the following sections is to compare the results of numerical simulations in two very different approaches to PBH formation in spherical symmetry. The one uses the CMC slicing with the conformally flat spatial coordinates, while the other uses the comoving slicing with the comoving threading, which is called the Misner-Sharp formulation of the Einstein equation in spherical symmetry with a perfect fluid. For this reason, we review the two formulations of the Einstein equations in spherical symmetry.

A. Gauge conditions in the two approaches

Shibata and Sasaki [9] adopt the conformally flat spatial coordinates. The line element is given by [34]

$$ds^2 = -(\alpha^2 - \psi^4 a^2 \beta^2 r^2) dt^2 + 2\psi^4 a^2 \beta r dr dt$$
$$+ \psi^4 a^2 (dr^2 + r^2 d\Omega^2), \qquad (5.1)$$

where $d\Omega^2 = d\theta^2 + \sin^2\theta d\phi^2$ is the line element on the unit two-sphere. Thence, we have $\beta^r = r\beta$ and $\tilde{\gamma}_{ij} = \eta_{ij}$.

The spatial metric is conformally flat and this is also a minimal distortion gauge because $\dot{\tilde{\gamma}}_{ij} = 0$. As for the slicing condition, Shibata and Sasaki [9] adopt the CMC slicing on which $K = -3H_b(t)$ and formulated the initial value problem of the Einstein equation. The combination of the conformally flat spatial coordinates and the CMC slicing fixes the gauge. Since the full set of field equations can be derived from the equations in Sec. II B and are given in Shibata and Sasaki [9], we do not repeat them here.

If we adopt the comoving slicing with the comoving threading, we have a compact set of field equations and this is called the Misner-Sharp formulation [35]. The line element is given by

$$ds^2 = -\alpha^2 dt^2 + b^2 dr^2 + R^2 d\Omega^2. \qquad (5.2)$$

The following equations derive from Eqs. (2.5), (2.6), (2.7), (2.8), (2.11), (2.12), (2.20) and (2.21) with $\beta^i = v^i = 0$:

$$M' = 4\pi \rho R^2 R', \qquad (5.3)$$

$$\dot{M} = -4\pi p R^2 \dot{R}, \qquad (5.4)$$

$$\dot{R}' = \dot{R}\frac{\alpha'}{\alpha} + R'\frac{\dot{b}}{b}, \qquad (5.5)$$

$$p' = -(\rho + p)\frac{\alpha'}{\alpha} \qquad (5.6)$$

$$M = \frac{R}{2}\left[1 - \frac{(R')^2}{b^2} + \frac{(\dot{R})^2}{\alpha^2}\right], \qquad (5.7)$$

where the prime denotes the partial derivative with respect to r and M is called the Misner-Sharp mass [35]. This formulation has been adopted for PBH studies by many authors including Polnarev and Musco [11].

B. Areal radius, mass excess and compaction function

In spherical symmetry, the areal radius is defined by $R = \sqrt{A/(4\pi)}$, where A is the area of the 2-sphere with constant t and r. We define the Kodama vector K^A by $K^A = \epsilon^{AB}\partial_B R$, where ϵ_{AB} is the totally antisymmetric tensor in the two-dimensional manifold charted by t and r and the Latin uppercase indices run over 0 and 1, and ϵ_{AB} is given by $\epsilon_{AB} = \sqrt{-G}\varepsilon_{AB}$ with the Levi-Civita symbol ε_{AB} and the determinant G of the two-dimensional metric G_{AB}. We raise the indices of ϵ_{AB} as $\epsilon_A{}^B = \epsilon_{AC}G^{CB}$ and $\epsilon^{AB} = G^{AC}\epsilon_C{}^B$. We trivially extend K^A to K^μ as a vector field in the four-dimensional manifold. Since $S^\mu = T^\mu_\nu K^\nu$ is a conserved current,

$$M := -\int S^\mu d\Sigma_\mu = -\int S^\mu n_\mu d\Sigma = \int S^t \alpha\sqrt{\gamma}dx^3 \quad (5.8)$$

is a conserved mass, where in the last expression Σ is chosen to the constant t hypersurface and the integration is done within a ball on Σ. M is called the Kodama mass. This is equivalent to the Misner-Sharp mass in the present setting.

Shibata and Sasaki [9] introduce the notion of a compaction function. Here we define it in more general settings. To this end we first define an excess δM in the Kodama mass by the difference between the Kodama masses of the two spheres of same t and *areal radius R* (not r) in two different spherically symmetric spacetimes. This definition of δM is covariant with respect to the choice of spatial coordinates but does depend on the slicing. We use the flat FRW spacetime as a reference spacetime to define the mass excess.

In an analogy with asymptotic flatness, if initial data approach those of the flat FRW one so fast that the mass excess has a finite limit as we take $r \to \infty$, we call such data *asymptotically flat FRW*. For asymptotically flat FRW data, if the mass excess approaches zero as we take $r \to \infty$, we shall call such initial data *compensated*; otherwise, we shall call it *uncompensated*. It is not clear which model is more physically realistic, compensated or uncompensated. Clearly, uncompensated models are more generic than the compensated ones. Physics should be as generic as possible within the framework of asymptotically flat FRW data. On the other hand, uncompensated models might be regarded as perturbations of infinitely long wavelength.

We define a compaction function $\mathcal{C}(t, r)$ by the ratio of the mass excess to the common areal radius of the two spheres, i.e.,

$$\mathcal{C}(t, r) := \frac{\delta M(t, r)}{R(t, r)}. \qquad (5.9)$$

By definition, $\mathcal{C}(t, r) = 0$ for the flat FRW spacetime. For asymptotically flat FRW data, we find $\mathcal{C} \propto 1/R$ as we fix t and take the limit $r \to \infty$. In the following we express the compaction function in terms of the density perturbation first in the Misner-Sharp formulation and later in more general slicings.

1. Comoving slicing

In the Misner-Sharp formulation, for which the line element is given in the form of Eq. (5.2), the components K^μ of the Kodama vector are given by

$$K^t = -\frac{R'}{\alpha b}, \qquad K^r = \frac{\dot{R}}{\alpha b}, \qquad K^\theta = K^\phi = 0. \quad (5.10)$$

Then, we find

$$S^t = T^t_\mu K^\mu = T^t_t K^t = \frac{R'}{\alpha b}\rho, \qquad (5.11)$$

where we have used $u_i = 0$ in this coordinate system, and hence

$$M(t, r) = 4\pi \int_0^r dx \rho R^2(t, x) R'(t, x). \tag{5.12}$$

Note that this expression is fully valid even in the general spherically symmetric spacetime and shows the equivalence between the Kodama mass and the Misner-Sharp mass. We denote the Kodama mass in the flat FRW spacetime by M_F, which is given by

$$M_F(t, r) = 4\pi \rho_b a^3 \int_0^r dx x^2. \tag{5.13}$$

Then the mass excess is defined by

$$\delta M(t, r) := M(t, r) - M_F(t, \tilde{r}), \tag{5.14}$$

where $\tilde{r}$ in the FRW spacetime gives the same areal radius $R(t, r)$ of the sphere of r on the constant t hypersurface in the perturbed spacetime, namely,

$$a(t)\tilde{r} = R(t, r). \tag{5.15}$$

Since Σ is the constant t hypersurface in both unperturbed and perturbed spacetimes, we find

$$a(t)d\tilde{r} = R'(t, r)dr, \tag{5.16}$$

therefore,

$$M_F(t, \tilde{r}) = 4\pi \rho_b \int_0^r dx R^2(t, x) R'(t, x). \tag{5.17}$$

Thus, we find the following exact relation,

$$\delta M(t, r) = 4\pi \rho_b \int_0^r dx R^2(t, x) R'(t, x) \delta(t, x), \tag{5.18}$$

where

$$\delta := \frac{\rho - \rho_b}{\rho_b}. \tag{5.19}$$

This is independent of the choice of the spatial coordinates. Thus, we have established the theorem that in spherical symmetry and in the comoving slicing, the density perturbation integrated over the perturbed spatial geometry exactly coincides with the mass excess. We can also have the exact expression for the compaction function as follows,

$$\mathcal{C} = \frac{1}{2}\bar{\delta}(H_b R)^2, \tag{5.20}$$

where the averaged density perturbation $\bar{\delta}$ is defined as

$$\bar{\delta}(t, r) := \frac{\int \delta d\Sigma}{\int d\Sigma} = \frac{4\pi \int_0^r dx R^2(t, x) R'(t, x) \delta(t, x)}{4\pi \int_0^r dx R^2(t, x) R'(t, x)} \tag{5.21}$$

with the spatial integration in the perturbed metric and the Friedmann equation (4.7) is used.

2. General time slicing

Next we will see the situation in the general time slicing with the conformally flat spatial coordinates, for which the line element is given in the form of Eq. (5.1). Then, R is given by

$$R = \psi^2 ar, \tag{5.22}$$

and the Kodama mass is given by

$$M(t, r) = 4\pi \int_0^r dx x^2 a^3 \alpha \psi^6 T^t_\mu K^\mu \tag{5.23}$$

from Eq. (5.8). Since K^μ are given by [34]

$$K^t = -\frac{1}{\alpha \psi^2}(\psi^2 r)', \quad K^r = \frac{r}{\alpha \psi^2 a}(\psi^2 a)_{,t},$$

$$K^\theta = K^\phi = 0, \tag{5.24}$$

M is expressed as

$$M(t, r) = 4\pi a^3 \int_0^r dx x^2 \psi^4 \{-[(\rho + p)u^t u_t + p](\psi^2 x)' + (\rho + p)u^t u_r \frac{x}{a}(\psi^2 a)_{,t}\}. \tag{5.25}$$

In the flat FRW spacetime, this reduces to

$$M_F(t, r) = 4\pi a^3 \rho_b \int_0^r dx x^2. \tag{5.26}$$

We have defined the mass excess $\delta M(t, r)$ as the difference between the Kodama masses enclosed in two spheres with the *same areal radius* in the perturbed spacetime and the FRW spacetime, i.e.,

$$\delta M(t, r) := M(t, r) - M_F(t, \psi^2 r). \tag{5.27}$$

Assuming the long-wavelength solutions, we find

$$M(t, r) = 4\pi a^3 \rho_b \int_0^r dx x^2 (1 + \delta)\psi^6 \left(1 + \frac{2r}{\psi}\psi'\right) + O(\epsilon^3), \tag{5.28}$$

while the integral in $M_F(t, \psi^2 r)$ can be transformed as follows,

$$\int_0^{\psi^2(t,r)r} dx x^2 = \int_0^{\varphi_t(r)} dx x^2 = \int_0^r dy \frac{d\varphi_t}{dy} \varphi_t^2$$
$$= \int_0^r dy y^2 \psi^6 \left(1 + \frac{2y}{\psi} \psi'\right), \qquad (5.29)$$

where $\varphi_t(r) := \psi^2(t,r)r$. Therefore, we find

$$\delta M = 4\pi a^3 \rho_b \int_0^r dx x^2 \psi^6 \left(1 + \frac{2x}{\psi} \psi'\right) \delta + O(\epsilon^3). \qquad (5.30)$$

Thus, we have established the theorem that the density perturbation integrated over the perturbed spacetime coincides with the mass excess to $O(\epsilon^2)$ in any time slicing which is compatible with the long-wavelength scheme. The compaction function satisfies

$$\mathcal{C} = \frac{1}{2} \bar{\delta} (H_b R)^2 + O(\epsilon^3). \qquad (5.31)$$

We can confirm that in the comoving slicing, where $u_r = 0$, Eqs. (5.30) and (5.31) hold without the term of $O(\epsilon^3)$ on the right-hand side.

VI. SPHERICALLY SYMMETRIC COSMOLOGICAL PERTURBATIONS

A. Long-wavelength solutions

Now that we have the long-wavelength solutions without symmetry in Sec. IV, it is straightforward to apply those to spherical symmetry. For convenience, we use the spherical coordinates in which the flat metric η_{ij} takes the following form:

$$\eta_{ij} dx^i dx^j = dr^2 + r^2(d\theta^2 + \sin^2\theta d\phi^2). \qquad (6.1)$$

In the CMC slicing, the solution is given by Eqs. (4.31), (4.32), (4.45)–(4.50), where the expressions for ξ, v_j and h_{ij} hold only for the normal coordinates and

$$\Psi = \Psi(r), \qquad (6.2)$$

$$f = -\frac{4}{3} \frac{1}{\Psi^5} \frac{1}{r^2} \frac{d}{dr} \left(r^2 \frac{d\Psi}{dr}\right), \qquad (6.3)$$

$$p_{ij} = \frac{1}{\Psi^4} \left[-\frac{2}{\Psi} \left(\bar{\mathcal{D}}_i \bar{\mathcal{D}}_j \Psi - \frac{1}{3} \eta_{ij} \bar{\Delta} \Psi\right) \right.$$
$$\left. + \frac{6}{\Psi^2} \left(\bar{\mathcal{D}}_i \Psi \bar{\mathcal{D}}_j \Psi - \frac{1}{3} \eta_{ij} \bar{\mathcal{D}}^k \Psi \bar{\mathcal{D}}_k \Psi\right)\right]. \qquad (6.4)$$

In the comoving slicing, the solution is given by Eqs. (4.31), (4.32), (4.68)–(4.73), where the expressions

for ξ, v_j and h_{ij} are valid in the normal coordinates and f and p_{ij} are given by Eqs. (6.2)–(6.4).

B. Asymptotic quasihomogeneous solutions

Polnarev and Musco [11] presented asymptotic quasihomogeneous solutions as cosmological nonlinear perturbations based on the Misner-Sharp formulation. We briefly review these solutions below.

We choose the flat FRW spacetime as the reference spacetime, which is given by Eq. (5.2) with

$$\alpha = 1, \qquad b = a(t), \qquad R = a(t)r = R_b(t,r),$$
$$\rho = \rho_b(t), \qquad M = M_b := \frac{4\pi \rho_b R_b^3}{3},$$
$$U = \dot{a}r = H_b R_b, \qquad H_b = \frac{\dot{a}}{a},$$

where $U := \dot{R}/\alpha$. The line element is written in the form

$$ds^2 = -dt^2 + a^2(t)[dr^2 + r^2(d\theta^2 + \sin^2\theta d\phi^2)].$$

We define r_0 as the comoving scale under consideration. Then, $R_0 = a(t)r_0$ is the corresponding physical scale. We define

$$\varepsilon := \left(\frac{1}{H_b R_0}\right)^2 = \left(\frac{1}{\dot{a}r_0}\right)^2 = \left(\frac{1}{H_b a r_0}\right)^2. \qquad (6.5)$$

Note that ε is time dependent and

$$\frac{\dot{\varepsilon}}{\varepsilon} = (3\Gamma - 2)H_b \qquad (6.6)$$

implies that ε increases in time if $\Gamma > 2/3$. The correspondence between the Shibata-Sasaki ϵ and Polnarev-Musco ε is thus given by $\epsilon^2 \sim \varepsilon$, although the perturbation scheme is somewhat different; Polnarev and Musco [11] introduce ε as a small time-dependent function, while Shibata and Sasaki [9] introduce ϵ as a constant order parameter which controls the order of spatial gradients at the fixed time and which is finally taken to be unity after the expansion.

As for nonlinear cosmological fluctuations, we assume that the metric approaches

$$ds^2 = -dt^2 + a^2(t) \left[\frac{dr^2}{1 - K(r)r^2} + r^2(d\theta^2 + \sin^2\theta d\phi^2)\right] \qquad (6.7)$$

in the limit $\varepsilon \to 0$ and expand α, b, R, ρ, U and M as

$$\alpha = 1 + \varepsilon \tilde{\alpha}, \qquad b = \frac{R'}{\sqrt{1 - K(r)r^2}}(1 + \varepsilon \tilde{b}), \qquad R = R_b(1 + \varepsilon \tilde{R}),$$

$$\rho = \rho_b(1 + \varepsilon \tilde{\rho}), \qquad U = H_b R(1 + \varepsilon \tilde{U}), \qquad M = \frac{4\pi}{3}\rho_b R^3(1 + \varepsilon \tilde{M}),$$

noting that $K(r) = O(\epsilon^0)$. We expand the Einstein equations (5.3)–(5.7) in a power series of ε. We can find that the first-order functions can be written in terms of $K(r)$ through Eq. (5.7). The concrete expressions are as follows,

$$\tilde{\alpha} = -\frac{3(\Gamma - 1)}{3\Gamma + 2}\frac{(r^3 K(r))'}{3r^2}r_0^2 + O(\varepsilon), \qquad (6.8)$$

$$\tilde{b} = \frac{3(\Gamma - 1)}{(3\Gamma - 2)(3\Gamma + 2)}r\left[\frac{(r^3 K(r))'}{3r^2}\right]' r_0^2 + O(\varepsilon), \qquad (6.9)$$

$$\tilde{R} = -\frac{1}{(3\Gamma - 2)(3\Gamma + 2)}\left[(\Gamma - 1)\frac{(r^3 K(r))'}{r^2} + K(r)\right]r_0^2 + O(\varepsilon), \qquad (6.10)$$

$$\tilde{\rho} = \frac{3\Gamma}{3\Gamma + 2}\frac{(r^3 K(r))'}{3r^2}r_0^2 + O(\varepsilon), \qquad (6.11)$$

$$\tilde{M} = \frac{3\Gamma}{3\Gamma + 2}K(r)r_0^2 + O(\varepsilon), \qquad (6.12)$$

$$\tilde{U} = -\frac{1}{3\Gamma + 2}K(r)r_0^2 + O(\varepsilon), \qquad (6.13)$$

where we have dropped a decaying mode.

The density perturbation $\bar{\delta}(t, r)$ averaged over the region inside the sphere of the radius r is calculated as

$$\bar{\delta}(t, r) = \varepsilon\frac{3\Gamma}{3\Gamma + 2}K(r)r_0^2 + O(\varepsilon^2). \qquad (6.14)$$

Expanding $\bar{\delta}(t, r)$ as $\bar{\delta}(t, r) = \varepsilon\tilde{\bar{\delta}}(t, r)$, we find

$$\tilde{\bar{\delta}}(t, r) = \frac{3\Gamma}{3\Gamma + 2}K(r)r_0^2 + O(\varepsilon), \qquad (6.15)$$

which is time independent in the limit $\varepsilon \to 0$. This coincides with the mass perturbation $\tilde{M}(t, r)$ to $O(\varepsilon^0)$, i.e., $\tilde{\bar{\delta}} = \tilde{M} + O(\varepsilon)$. This is consistent with the full-order equation (5.20) noting $M_b = H_b^2 R_b^3/2$ and $R_b = ar$.

For variable equations of state and for more general modes, see Polnarev and Musco [11]. For higher-order solutions with respect to ε, see Polnarev et al. [14].

C. Equivalence of the two solutions

As we have seen in Sec. III C, the CMC slicing and comoving slicing coincide with each other to $O(\epsilon)$. This means that the spatial metrics $d\Sigma^2$ in these slicings are identical to $O(\epsilon)$. In the conformally flat coordinates, the spatial metric is given by

$$d\Sigma^2 = a^2(t)\Psi^4(\varpi)[d\varpi^2 + \varpi^2(d\theta^2 + \sin^2\theta d\phi^2)] + O(\epsilon^2),$$

while in the areal radial coordinates, it is given by

$$d\Sigma^2 = a^2(t)\left[\frac{dr^2}{1 - K(r)r^2} + r^2(d\theta^2 + \sin^2\theta d\phi^2)\right] + O(\epsilon^2),$$

where and, hereafter, we denote the radial coordinate in the conformally flat spatial coordinates with ϖ to distinguish between the two coordinates. The former and the latter are adopted by Shibata and Sasaki [9] and Polnarev and Musco [11], respectively. The coincidence of the two metrics implies the following relations:

$$\begin{cases} \Psi(\varpi)^2 d\varpi = \frac{dr}{\sqrt{1 - K(r)r^2}}, \\ \Psi(\varpi)^2\varpi = r. \end{cases} \qquad (6.16)$$

The above expression can be inverted for r and $K(r)$ in terms of ϖ and $\Psi(\varpi)$ as

$$\begin{cases} r = \Psi^2(\varpi)\varpi, \\ K(r)r^2 = 1 - \left(1 + 2\frac{\varpi}{\Psi(\varpi)}\frac{d\Psi(\varpi)}{d\varpi}\right)^2. \end{cases} \qquad (6.17)$$

Using Eqs. (6.16) and (6.17), we can prove the following relation:

$$\frac{1}{3}\frac{1}{r^2}\frac{d(r^3 K(r))}{dr} = -\frac{4}{3}\frac{1}{\varpi^2\Psi^5}\frac{d}{d\varpi}\left(\varpi^2\frac{d\Psi}{d\varpi}\right). \qquad (6.18)$$

Let us prove this identity. From Eq. (6.17), we find

$$\sqrt{1 - K(r)r^2} = 1 + 2\varpi\frac{1}{\Psi}\frac{d\Psi}{d\varpi}.$$

Together with Eq. (6.16), we find

$$\frac{1}{3r^2}\frac{d}{dr} = \frac{1}{3\varpi^2\Psi^5(\Psi + 2\varpi\frac{d\Psi}{d\varpi})}\frac{d}{d\varpi}.$$

On the other hand, we find

$$r^3 K(r) = -4\varpi^2\frac{d\Psi}{d\varpi}\left(\Psi + \varpi\frac{d\Psi}{d\varpi}\right). \tag{6.19}$$

Differentiating the right-hand side with respect to ϖ, we find

$$\frac{d}{d\varpi}\left[\varpi^2\frac{d\Psi}{d\varpi}\left(\Psi + \varpi\frac{d\Psi}{d\varpi}\right)\right]$$
$$= \left(\Psi + 2\varpi\frac{d\Psi}{d\varpi}\right)\frac{d}{d\varpi}\left(\varpi^2\frac{d\Psi}{d\varpi}\right).$$

From the above equations, we finally obtain Eq. (6.18).
From Eqs. (6.3) and (6.18), we find a useful relation,

$$f = \frac{1}{3r^2}\frac{d}{dr}(r^3 K(r)). \tag{6.20}$$

Equations (6.16) can be integrated to give ϖ and $\Psi(\varpi)$ in terms of r and $K(r)$ as

$$\begin{cases} \varpi = r\exp\left[\int_\infty^r \frac{dx}{x}\left(\frac{1}{\sqrt{1 - K(x)x^2}} - 1\right)\right], \\ \Psi(\varpi) = \exp\left[-\frac{1}{2}\int_\infty^r \frac{dx}{x}\left(\frac{1}{\sqrt{1 - K(x)x^2}} - 1\right)\right], \end{cases} \tag{6.21}$$

where for simplicity we have assumed

$$\lim_{r\to\infty} K(r)r^2 = 0, \qquad \lim_{\varpi\to\infty}\Psi(\varpi) = 1. \tag{6.22}$$

In spite of the above equivalence, it should be noted that the turning point where $K(r)r^2 = 1$, which is a coordinate singularity in the areal radial coordinates, can be overcome in the conformally flat coordinates as Kopp *et al.* [36] point out.

The correspondence between the Polnarev-Musco variables and Shibata-Sasaki variables is given by

$$\delta = \varepsilon\tilde\rho + O(\varepsilon^2), \tag{6.23}$$

$$\chi = \varepsilon\tilde\alpha + O(\varepsilon^2), \tag{6.24}$$

$$\kappa = -\varepsilon\frac{1}{3}[3\tilde\alpha - (3\Gamma - 2)(3\tilde R + r\tilde R' + \tilde b)] + O(\varepsilon^2). \tag{6.25}$$

Using the relation (6.20), we can see that the Polnarev-Musco asymptotic quasihomogeneous solutions given by Eqs. (6.8)–(6.11) are equivalent to the long-wavelength solutions in the comoving slicing given by Eqs. (4.68)–(4.70).

D. Correspondence relation between the two solutions

The difference between the Shibata-Sasaki and Polnarev-Musco formulations is in the choice of time slicing and spatial coordinates. In Eq. (4.82), we establish the correspondence relation

$$\delta_C = \frac{3\Gamma}{3\Gamma + 2}\delta_{\rm CMC} + O(\epsilon^4). \tag{6.26}$$

The prefactor on the right-hand side is due to the difference in time slicing. Note that Eq. (6.26) implies

$$\tilde{\bar\delta}_C = \frac{3\Gamma}{3\Gamma + 2}\tilde{\bar\delta}_{\rm CMC} + O(\epsilon^4), \tag{6.27}$$

where $\bar\delta_{\rm CMC} = \epsilon\tilde{\bar\delta}_{\rm CMC}$. In particular, we find the useful relation from Eqs. (6.15) and (6.27),

$$\tilde{\bar\delta}_{\rm CMC} = K(r)r_0^2 + O(\epsilon^2). \tag{6.28}$$

It is also interesting to derive the expressions for physical quantities in terms of both the Shibata-Sasaki variables and Polnarev-Musco variables. Shibata and Sasaki [9] measure the amplitude of the perturbation by $\Psi(0)$. This can be expressed in terms of the Polnarev-Musco variables as follows:

$$\Psi(0) = \exp\left[\frac{1}{2}\int_0^\infty \frac{dr}{r}\left(\frac{1}{\sqrt{1 - K(r)r^2}} - 1\right)\right]. \tag{6.29}$$

Since

$$\delta M = 4\pi a^3\rho_b\int_0^\varpi dx x^2\Psi^6\left(1 + \frac{2x}{\Psi}\frac{d\Psi}{dx}\right)\delta + O(\epsilon^3), \tag{6.30}$$

in both slicings, Eq. (6.26) implies

$$\delta M_C = \frac{3\Gamma}{3\Gamma + 2}\delta M_{\rm CMC} + O(\epsilon^3). \tag{6.31}$$

For the CMC slicing, substituting Eqs. (4.45) and (6.3) into Eq. (6.30), we find

$$\delta M_{\rm CMC} = \frac{4\pi a^3\rho_b}{3a^2 H_b^2}\int_0^\varpi dx(-4)x(2\Psi' + x\Psi'')(\Psi + 2x\Psi')$$
$$+ O(\epsilon^3)$$
$$= -2a\varpi^2\Psi'(\Psi + \varpi\Psi') + O(\epsilon^3). \tag{6.32}$$

Therefore, the mass excess uniformly increases in proportion to the scale factor. The compaction function $\mathcal{C}$ is then calculated as follows:

$$\mathcal{C}_{\mathrm{CMC}} = \frac{\delta M_{\mathrm{CMC}}}{\varpi \Psi^2 a} = \frac{1}{2}\left[1 - \left(1 + 2\frac{\varpi}{\Psi}\frac{d\Psi}{d\varpi}\right)^2\right] + O(\epsilon^3).$$

$$(6.33)$$

This is time independent to $O(\epsilon^2)$. From Eq. (6.31), we have

$$\mathcal{C}_C = \frac{3\Gamma}{3\Gamma + 2}\mathcal{C}_{\mathrm{CMC}} + O(\epsilon^3). \qquad (6.34)$$

From Eqs. (6.17) and (6.33), we find a very simple relation:

$$\mathcal{C}_{\mathrm{CMC}} = \frac{1}{2}K(r)r^2 + O(\epsilon^3). \qquad (6.35)$$

Hence, from Eqs. (6.15) and (6.27), the relation between $\tilde{\tilde{\delta}}$ and the compaction function $\mathcal{C}$ is given by

$$\mathcal{C} = \frac{1}{2}\tilde{\tilde{\delta}}(r)\left(\frac{r}{r_0}\right)^2 + O(\epsilon^3), \qquad (6.36)$$

and, in particular,

$$\mathcal{C}(t, r_0) = \frac{1}{2}\tilde{\tilde{\delta}}(r_0) + O(\epsilon^3) \qquad (6.37)$$

in any slicing. In fact, we can see that Eqs. (6.36) and (6.37) directly follow from Eqs. (5.20) and (5.31).

Before moving onto the comparison of the numerical results, we show how the asymptotic condition restricts the functions $\Psi(\varpi)$ and $K(r)$. If we assume $\Psi(\varpi) \to 1$ and $K(r)r^2 \to 0$ in the asymptotic region, from Eq. (6.33), the asymptotic flat FRW condition implies $\Psi - 1 = O(1/\varpi)$, while the compensation condition implies faster falloff. If we assume $\Psi = 1 + C_\psi/(2\varpi) + O(1/\varpi^2)$, we find

$$\lim_{r \to \infty} \delta M_{\mathrm{CMC}} = aC_\psi, \qquad \mathcal{C}_{\mathrm{CMC}} \approx \frac{C_\psi}{\varpi}. \qquad (6.38)$$

The compensated model corresponds to $C_\psi = 0$. In terms of $K(r)$, we find the asymptotic flat FRW condition implies $K(r) = O(1/r^3)$, while the compensation condition implies faster falloff. If we assume $K(r) = 2C_K/r^3 + O(1/r^4)$, we find

$$\lim_{r \to \infty} \delta M_{\mathrm{CMC}} = aC_K, \qquad \mathcal{C}_{\mathrm{CMC}} \approx \frac{C_K}{r}. \qquad (6.39)$$

The compensated model corresponds to $C_K = 0$.

VII. NUMERICAL RESULTS

A. Setup of numerical simulations

In the decelerated expansion, such as in the radiation-dominated era, the Hubble horizon expands in terms of the comoving scale. In this phase, primordial cosmological perturbations which were on superhorizon scale enter within the Hubble scale, which is called horizon entry. Much before the horizon entry, such primordial cosmological perturbations are naturally described by the long-wavelength solutions. The argument of Jeans instability strongly suggests that the density perturbation which collapses to a black hole must be of order unity at horizon entry because the Jeans scale is comparable with the Hubble scale if $\Gamma - 1 = O(1)$. Since $\bar{\tilde{\delta}}(r_0)$ approximately gives the averaged density perturbation at horizon entry, the discussion in Sec. VI D implies that the compaction function $\mathcal{C}$ and the curvature variable Ψ must have been perturbed by order of unity even much before the horizon entry. Thus, it is natural to prepare the nonlinear long-wavelength solutions as initial data sets for PBH formation at the moment much before the horizon entry.

As we have seen, there are two major approaches, the one is adopted by Shibata and Sasaki [9] and the other is adopted by Polnarev and Musco [11]. They are different not only in time slicing and spatial coordinates but also in amplitude measures and in initial curvature profiles, which lead to the complexity in the comparison of the numerical results between these two approaches. Since we have already discussed the formulations, we will focus on the difference in initial curvature profiles. Shibata and Sasaki [9] determine the initial data by performing iteration to solve the Hamiltonian and momentum constraints with the conformally flat spatial coordinates so that the density profile is given by

$$\psi^6 \delta_{\mathrm{CMC}}$$

$$= C_\delta\left[\exp\left(-\frac{\varpi^2}{\varpi_0^2}\right) - \sigma^{-3}\exp\left(-\frac{\varpi^2}{\sigma^2\varpi_0^2}\right)\right]\left(\frac{t}{\varpi_0}\right)^{2-\frac{4}{3\Gamma}},$$

$$(7.1)$$

with the boundary condition

$$\psi = 1 + \frac{C_\psi}{2\varpi} + O(\varpi^{-2}) \qquad (7.2)$$

as $\varpi \to \infty$, while δ_{CMC} and $u_{j\,\mathrm{CMC}}$ are those for the long-wavelength solutions, i.e., Eqs. (4.45) and (4.48). ϖ_0 is fixed and then σ and C_δ parametrize the profiles. Note that the above model is approximately compensated because the overdensity in the first term and the underdensity in the second term in the square brackets on the right-hand side of Eq. (7.1) cancel out if they are integrated over the whole flat space with $\psi = 1$. However, since the space is not flat or ψ is not identically unity, this model is generally uncompensated. Another complexity comes from the different amplitude measures. Shibata and Sasaki [9] adopt $\Psi(0)$ and $\mathcal{C}_{\mathrm{CMC,max}}$ as amplitude measures, where $\mathcal{C}_{\mathrm{CMC,max}}$ is the maximum value of $\mathcal{C}_{\mathrm{CMC}}$.

Polnarev and Musco [14] and Musco and Miller [13] give Gaussian-type profiles and top-hat-type profiles. In both cases, the profiles fall off much faster than r^{-3} as $r \to \infty$ and hence their profiles correspond to exactly compensated models. In the Gaussian type, $K(r)$ is given by

$$K(r) = \left(1 + \alpha \frac{r^2}{2\Delta^2}\right) \exp\left(-\frac{r^2}{2\Delta^2}\right), \qquad (7.3)$$

which is parametrized by Δ and α. They adopt $\tilde{\tilde{\delta}}_{C,0} := \tilde{\tilde{\delta}}_C(r_0)$ as an amplitude measure, where r_0 is specified as the smallest positive root of $\tilde{\rho}(r) = 0$. We will abbreviate $\Psi(0)$, $\mathcal{C}_{\mathrm{CMC,max}}$ and $\tilde{\tilde{\delta}}_{C,0}$ as ψ_0, $\mathcal{C}_{\mathrm{max}}$ and $\tilde{\delta}$, respectively.

Hereafter we only keep the lowest order terms and neglect higher order terms in terms of ϵ of the long-wavelength solutions as initial data sets because this truncation is numerically justified if ϵ is sufficiently small in Polnarev and Musco [11]. Equation (6.11) implies that r_0 is a positive root of the equation $(r^3 K(r))' = 0$, while Eq. (6.35) implies that r_1 is a positive root of the equation $(r^2 K(r))' = 0$, where $r = r_1$ is the radius at which $\mathcal{C}_{\mathrm{CMC}}$ takes a maximum. If we assume a top-hat shape for $K(r)$, we can see $r_0 = r_1$ and, hence,

$$\mathcal{C}_{\mathrm{max}} = \frac{3\Gamma + 2}{6\Gamma} \tilde{\delta}. \qquad (7.4)$$

In Sec. VIII C, we will see the top-hat curvature model in more detail. For an exact Gaussian model, where

$$K(r) = \exp\left(-\frac{r^2}{2\Delta^2}\right), \qquad (7.5)$$

we find $r_0 = \sqrt{3}\Delta$ and $r_1 = \sqrt{2}\Delta$ and hence

$$\mathcal{C}_{\mathrm{max}} = \frac{3\Gamma + 2}{9\Gamma} \sqrt{e}\tilde{\delta}. \qquad (7.6)$$

Note that the above relation is justified only for the exact Gaussian profile for $K(r)$. There is no one-to-one correspondence between ψ_0, $\mathcal{C}_{\mathrm{max}}$ and $\tilde{\delta}$ unless we specify the profile.

B. Comparison of the numerical results

To test the consistency between the results of Shibata and Sasaki [9] and the results of Polnarev and Musco [11] and Musco and Miller [13], we will reproduce the former simulation with the latter formulation. The matter field is assumed to be a radiation fluid; i.e., $\Gamma = 4/3$ in this subsection.

To make discussion clearer, we first integrate

$$\frac{1}{\varpi^2 \Psi^5} \frac{d}{d\varpi}\left(\varpi^2 \frac{d\Psi}{d\varpi}\right) = -2\pi a^2 \rho_b \delta_{\mathrm{CMC}}, \qquad (7.7)$$

which is obtained by Eqs. (4.45) and (6.2), with the source term

$$\Psi^6 \delta_{\mathrm{CMC}}$$
$$= C_\delta\left[\exp\left(-\frac{\varpi^2}{\varpi_0^2}\right) - \sigma^{-3}\exp\left(-\frac{\varpi^2}{\sigma^2\varpi_0^2}\right)\right]\left(\frac{t}{\varpi_0}\right)^{2-\frac{4}{3\Gamma}}, \qquad (7.8)$$

and the boundary condition,

$$\Psi = 1 + \frac{C_\psi}{2\varpi} + O(\varpi^{-2}), \qquad (7.9)$$

as $\varpi \to \infty$. Then, we determine $K(r)$ through Eqs. (6.17). Equivalently, one may define $h(r) := \varpi(r)/r$ and solve

$$h'' + \frac{h'^2}{2h}\left(1 + \frac{rh'}{h}\right) + \frac{2h'}{r}$$
$$= \frac{3C_\delta}{8} h(rh)'^3\left[\exp(-r^2 h^2) - \sigma^{-3}\exp\left(-\frac{r^2 h^2}{\sigma^2}\right)\right], \qquad (7.10)$$

with the boundary condition $h = 1 - C_\psi/r + O(r^{-2})$ as $r \to \infty$. It would be useful to note that $h(0) = \Psi(0)^{-2}$. Then, $K(r)$ can be calculated by

$$K(r) = \frac{1}{r^2}\left(1 - \frac{h(r)^2}{(rh(r))'^2}\right). \qquad (7.11)$$

The obtained $K(r)$ generates asymptotic quasihomogeneous solutions given in Sec. VI B and we implement numerical simulations based on the Misner-Sharp formulation adopting those solutions as initial data sets. Several examples of the initial data sets for both $\Psi(\varpi)$ and $K(r)$ at the black hole threshold are plotted in Fig. 1 for different values of σ. The initial data sets constructed here are identical with those in Shibata and Sasaki [9] to $O(\epsilon)$.

The details of the numerical code are described in Nakama *et al.* [15]. The threshold models for black hole formation for different values of σ are summarized in Table I and Fig. 2, where the scales are chosen so that $a = a_f t^{\frac{2}{3\Gamma}}$, $a_f = 1$ and $\varpi_0 = 1$. We can see that the obtained numerical results are fairly consistent with Shibata and Sasaki [9]'s results by comparing their Figs. 2 and 7 with our Table I. Note that Shibata and Sasaki [9] estimate that the threshold value of ψ_0 is $\simeq 1.79$ in the limit $\sigma \to \infty$. Here we have also calculated and listed
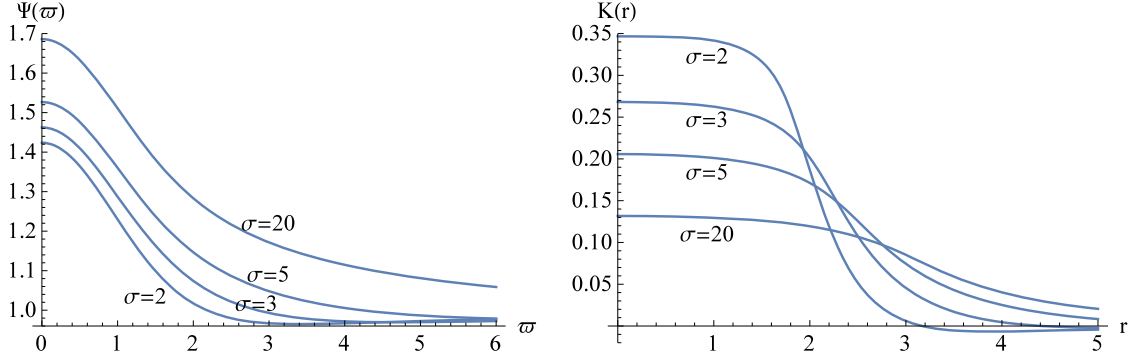
FIG. 1 (color online).   Initial profiles at black hole threshold for the model given by Eq. (7.8) with the different values of σ in terms of $\Psi(\varpi)$ (left panel) and $K(r)$ (right panel).

the values for C_ψ and $\tilde{\delta}$. We can see that C_ψ is negative for these threshold models, implying that the models are overcompensated. In fact, we have numerically found that C_ψ is negative also for all nonthreshold models we have calculated for $1.25 \leq \sigma \leq 20$. The threshold values of $\tilde{\delta}$ are comparable with those obtained by Polnarev and Musco [11] and Musco and Miller [13].

It is also interesting to calculate ψ_0 and $C_{\max}$ for the results of Polnarev and Musco [11] and Musco and Miller [13]. In fact, this is possible without reproducing the numerical simulations because the initial profiles in Polnarev-Musco and Musco-Miller simulations are given explicitly in terms of elementary functions. The results for the Gaussian-type profiles are summarized in Table II and Fig. 3.

C. Threshold values of $\tilde{\delta}$, $\mathcal{C}_{\max}$ and ψ_0

Hereafter, we denote the threshold values of $\tilde{\delta}$, $\mathcal{C}_{\max}$ and ψ_0 as $\tilde{\delta}_c$, $\mathcal{C}_{\max,c}$ and $\psi_{0,c}$, respectively. In Table I and Fig. 2, we can see that the larger the σ is, the smaller the $\tilde{\delta}_c$ becomes. This tendency is shared by $\mathcal{C}_{\max,c}$. This can be interpreted as follows. ϖ_0 gives the scale of the overdense region, while $\sigma\varpi_0$ gives that of the underdense region surrounding the overdense region and $-\sigma^{-3}$ gives the ratio of the density perturbation of scale $\sigma\varpi_0$ to the that of scale ϖ_0. If σ is not so larger than unity, the overdensity must be approximately compensated by the relatively narrow

underdense layer, resulting in a sharp transition to the background FRW universe (see Fig. 2). This enhances the effect of the pressure gradient and suppresses the gravitational collapse, resulting in the larger threshold values $\tilde{\delta}_c$ and $\mathcal{C}_{\max,c}$. If σ is much larger than unity, the underdense region spreads to large distances and hence the density there is only slightly lower than the FRW spacetime. Such a configuration minimizes the effect of pressure gradient force. This is the reason why $\tilde{\delta}_c$ and $\mathcal{C}_{\max,c}$ take minimum values $\simeq 0.42$ and $\simeq 0.38$, respectively, for $\sigma = 20$.

The same tendency can be seen also in the Gaussian-type profiles for $K(r)$ as seen in Table II and Fig. 3. The larger the α is, the larger the $\tilde{\delta}_c$ becomes. Figure 7 in Musco and Miller [13] shows that the larger the α is, the larger the density gradient and hence the pressure gradient become. The minimum value 0.45 of $\tilde{\delta}_c$ is realized for the pure Gaussian profile of $K(r)$, i.e., $\alpha = 0$. The factor $\sqrt{e}/2 \simeq 0.82$ in Eq. (7.6) explains the ratio of $\mathcal{C}_{\max,c} \simeq 0.37$ to $\tilde{\delta}_c \simeq 0.45$. As for the sharpest transition model, which is an approximately top-hat curvature model, Polnarev and
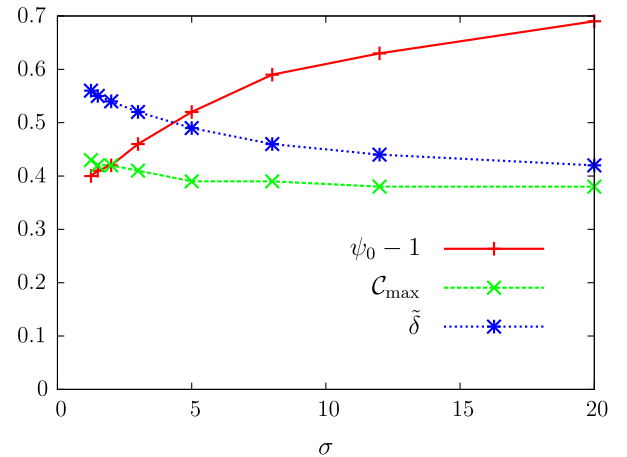

FIG. 2 (color online).   The threshold values of ψ_0, $\mathcal{C}_{\max}$ and $\tilde{\delta}$ for the model given by Eq. (7.8) for different values of σ.

TABLE I.   Black hole formation thresholds for the model given by Eq. (7.8) parametrized by σ and C_δ.

σ	1.25	1.5	2	3	5	8	12	20
C_δ	31.0	18.9	13.2	10.9	10.4	10.9	11.4	12.1
C_ψ	−0.22	−0.24	−0.28	−0.33	−0.41	−0.50	−0.57	−0.63
ψ_0	1.40	1.41	1.42	1.46	1.52	1.59	1.63	1.69
$\mathcal{C}_{\max}$	0.43	0.42	0.42	0.41	0.39	0.39	0.38	0.38
$\tilde{\delta}$	0.56	0.55	0.54	0.52	0.49	0.46	0.44	0.42

TABLE II.   Black hole formation thresholds for the model given by Eq. (7.3) parametrized by α and Δ.

α	0.00	0.25	0.50	0.75	1.00	2.00	5.00
Δ	1.01	0.89	0.80	0.73	0.68	0.54	0.36
r_0	1.75	1.70	1.61	1.51	1.42	1.15	0.80
r_1	1.43	1.40	1.35	1.29	1.22	1.01	0.71
ψ_0	1.61	1.59	1.57	1.57	1.55	1.53	1.50
$\mathcal{C}_{\max}$	0.37	0.37	0.38	0.38	0.39	0.39	0.40
$\tilde{\delta}$	0.45	0.46	0.47	0.47	0.48	0.49	0.50

Musco [11] even get $\tilde{\delta}_c \simeq 0.66$, which is nearly the possible maximum value $2/3$ of $\tilde{\delta}$ for the density perturbation [19].

On the other hand, the analytic threshold formula obtained in Harada *et al.* [19] yields $\tilde{\delta}_c \simeq 0.4135$ for a radiation fluid. One of the key assumptions to derive this analytic formula is that the effects of pressure gradient force due to the transition from the overdensity to the underdense layer can be neglected. From the above consideration, we can say that the analytic formula approximately gives the lowest value of $\tilde{\delta}_c$, which is realized if the transition between the overdense region and the FRW universe is sufficiently smooth.

For the equation of state $p = (\Gamma - 1)\rho$, the above discussion about the threshold of PBH formation in spherical symmetry is summarized as follows,

$$\tilde{\delta}_{c,\min} < \tilde{\delta}_c < \tilde{\delta}_{c,\max}, \qquad (7.12)$$

in the comoving slicing, where

$$\tilde{\delta}_{c,\min} \simeq \frac{3\Gamma}{3\Gamma + 2} \sin^2 \left(\frac{\pi\sqrt{\Gamma - 1}}{3\Gamma - 2} \right), \qquad (7.13)$$

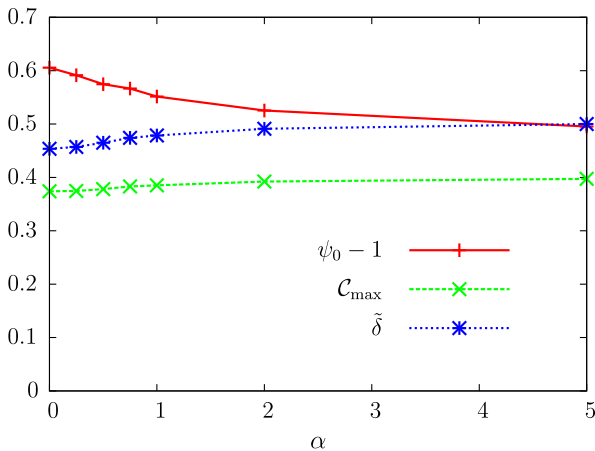$$\tilde{\delta}_{c,\max} \simeq \frac{3\Gamma}{3\Gamma + 2}. \qquad (7.14)$$

FIG. 3 (color online).   The threshold values of ψ_0, $\mathcal{C}_{\max}$ and $\tilde{\delta}$ for the model given by Eq. (7.3) with different values of α.

The smoother the transition from the overdensity to the FRW universe is, the smaller the $\tilde{\delta}_c$ becomes. The minimum value is realized if the transition is sufficiently smooth, while the maximum is realized if the transition is sufficiently sharp.

As seen in Tables I and II, it does not seem to affect $\tilde{\delta}_c$ and $\mathcal{C}_{\max,c}$ so much whether the model is compensated or not. This can be understood that the dynamics of black hole formation is determined within the background Hubble length and is not affected by a global mass excess. Both the amplitude measures $\tilde{\delta}$ and $\mathcal{C}_{\max}$ are quasilocal quantities and do not care about perturbations on scales much longer than the horizon scale at horizon entry.

On the other hand, we can see that $\psi_{0,c}$ shows a very different behavior from $\tilde{\delta}_c$ and $\mathcal{C}_{\max,c}$. In Table I and Fig. 2, we can see that as σ increases and hence the transition is smoother, $\psi_{0,c}$ *increases*. The same behavior is also seen in Table II and Fig. 3. As α increases and hence the transition is sharper, $\psi_{0,c}$ *decreases*. Based on this behavior, Shibata and Sasaki [9] conclude that if the overdensity is surrounded by a low density region, it efficiently collapses. We have confirmed that their conclusion is correct if one directly links the small $\psi_{0,c}$ to the efficient production of black holes, which should applies if the statistical or probability distribution of ψ_0 is regarded as fixed and is centered at its unperturbed value.

To elucidate why neither $\tilde{\delta}_c$ nor $\mathcal{C}_{\max}$ but $\psi_{0,c}$ significantly depends on the behavior of the surrounding region, it is helpful to recall that Ψ corresponds to the Newtonian potential for the density perturbation in the CMC slicing, which can be most clearly seen in Eq. (4.17) with $\kappa = 0$. The Newtonian potential contains the information of the surrounding region in contrast to the averaged density and the compaction function. For example, we can determine the averaged density and the compaction function at some radius r from the density distribution inside the sphere of radius r. On the contrary, to determine the Newtonian potential and its central value, we need the density distribution not only inside but also outside the sphere. Since the PBH formation threshold should be determined by dynamics inside the Hubble length, it would be most efficiently described by quasi-local quantities, such as $\bar{\delta}_c$ and $\mathcal{C}_{\max}$, rather than $\psi_{0,c}$. This is consistent with the suggestion by Young *et al.* [18].

At this stage it would be worthwhile to make several comments about the relationship between the arguments above and Nakama *et al.* [15]. This paper investigated the PBH formation condition for a much wider class of initial curvature profiles $K(r)$, which is described by a function with as many as five parameters, basically using the method of Polnarev and Musco [11]. This function mathematically includes (7.3) and also includes profiles which are very close to a top-hat, as well as profiles which are gentler than a Gaussian. In addition, that function was claimed to

include the profiles investigated by Shibata and Sasaki, characterized by Eq. (7.1), since the function turned out to fit the profiles of Shibata and Sasaki, after being translated into $K(r)$, fairly well with appropriate parameter choice. Actually that function was introduced partially in order to express gentler profiles as the ones investigated by Shibata and Sasaki, which are realized when σ is large. However, this statement about the inclusion may seem mathematically inaccurate since [15] also restricts attention to exactly compensated profiles, while Shibata and Sasaki's profiles are strictly speaking overcompensated as has been pointed out above. Still, that statement about the inclusion is physically justified since whether the initial perturbation is compensated or not does not affect the formation of PBHs that much, as has also been pointed out above.

Though the definition and physical meaning of $\tilde{\delta}$, along with the definition of r_0 as the radius of the overdensity, is clear and hence it is convenient, when one tries to discuss the PBH formation condition for more general profiles more precisely, it is also useful to introduce another phenomenological parameter characterizing the amplitude of initial perturbations instead of $\tilde{\delta}$, since $\tilde{\delta}$ is too sensitive to the information around r_0, which is expected not to affect the formation of PBHs that much. In [15] a parameter I was phenomenologically introduced, which is similar to $\tilde{\delta}$, as

well as Δ, which can be interpreted to measure pressure gradient force. It turned out that only these two parameters, characterizing perturbation profiles, are sufficient to describe the formation of PBHs quite well for the generalized class of curvature profiles specified by five parameters. In addition, the tendency mentioned above that $\tilde{\delta}_c$ is larger when the transition is sharper due to larger pressure gradient force, is also manifest in terms of these two crucial parameters I and Δ for the generalized profiles.

VIII. ANALYTIC RESULTS WITH SIMPLIFIED MODELS

A. Compensated top-hat density model: Physical interpretation

Here, we will see why $\psi_{0,c}$ behaves in the opposite way to $\tilde{\delta}_c$ and $\mathcal{C}_{\max,c}$. Since our purpose here is to understand this behavior qualitatively, we mimic the density profile model (7.1) by the following simple function,

$$\delta_{\mathrm{CMC}} = C_\delta[\Theta(r_0-r)-\sigma^{-3}\Theta(\sigma r_0-r)]\left(\frac{t}{r_0}\right)^{2-\frac{4}{3\Gamma}}, \quad (8.1)$$

where $\Theta(x)$ is Heaviside's step function. From Eq. (6.28), we find

$$K(r) = \begin{cases} C'_\delta(1-\sigma^{-3}) & (0 \leq r < r_0) \\ C'_\delta[(1-\sigma^{-3})r_0^3 - \sigma^{-3}(r^3-r_0^3)]/r^3 & (r_0 \leq r < \sigma r_0), \\ 0 & (r \geq \sigma r_0) \end{cases} \quad (8.2)$$

where we have put

$$C'_\delta := \frac{4}{9\Gamma^2}\frac{a_f^2}{r_0^{2-\frac{4}{3\Gamma}}}C_\delta. \quad (8.3)$$

We can see this model is exactly compensated and that r_0 and r_1 coincide with each other. For this model, we can find

$$\mathcal{C}_{\max} = \frac{1}{2}C'_\delta r_0^2(1-\sigma^{-3}), \quad (8.4)$$

$$\tilde{\delta} = \frac{3\Gamma}{3\Gamma+2}C'_\delta r_0^2(1-\sigma^{-3}). \quad (8.5)$$

On the other hand, by invoking the linear-order approximation in Eqs. (4.38) and (6.3), we obtain ψ_0 as

$$\psi_0 - 1 = \frac{3}{8}C'_\delta r_0^2(1-\sigma^{-1}). \quad (8.6)$$

We should note that $\psi_0 - 1$ depends on σ in quite a different manner from $\mathcal{C}_{\max}$ and $\tilde{\delta}$.

Although this model is very simple, it is still difficult to analytically obtain the black hole threshold. The density

gradient is initially infinite but it becomes finite immediately after the time evolution sets in, so that we have to take the balance between the gravitational force and the pressure gradient force into account in this highly dynamical system. Here, we make this model more phenomenological noting the intriguing dependence on σ. For this purpose, we introduce three positive constants of order unity, c_1, c_2 and c_3, to simply parametrize the profile dependence as well as nonlinearity.

$$\psi_0 - 1 = c_1\frac{3}{8}C'_\delta r_0^2(1-\sigma^{-1}), \quad (8.7)$$

$$\mathcal{C}_{\max} = c_2\frac{1}{2}C'_\delta r_0^2(1-\sigma^{-3}), \quad (8.8)$$

$$\tilde{\delta} = c_3\frac{3\Gamma}{3\Gamma+2}C'_\delta r_0^2(1-\sigma^{-3}), \quad (8.9)$$

These three parameters are unity for the top-hat density model (8.1). From the above equations, we can derive the following phenomenological relations:

$$\psi_0 - 1 = \frac{3}{4}\frac{c_1}{c_2}\frac{1-\sigma^{-1}}{1-\sigma^{-3}}\mathcal{C}_{\max} = \frac{c_1}{c_3}\frac{3\Gamma+2}{8\Gamma}\frac{1-\sigma^{-1}}{1-\sigma^{-3}}\tilde{\delta},$$

$$\mathcal{C}_{\max} = \frac{c_2}{c_3}\frac{3\Gamma+2}{6\Gamma}\tilde{\delta}. \tag{8.10}$$

Here we just assume that the σ dependence of $\tilde{\delta}_c$ and $\mathcal{C}_{\max,c}$ is very weak. Then, $\psi_{0,c}$ is a monotonically increasing function of σ for $\sigma > 1$. The above simplistic analysis explains the qualitative feature of the numerical results shown in Table I and Fig. 2 fairly well. In fact, if we choose

$$\frac{c_1}{c_2} \simeq 2.8, \qquad \frac{c_1}{c_3} \simeq 3 \tag{8.11}$$

the relations (8.10) agree with the numerical results in Fig. 2 qualitatively, although the numerical results are obtained by the model Eq. (7.8) and the Einstein equation is solved fully nonlinearly. The above discussion suggests that the formation criterion can be well described by the quasilocal quantities such as $\mathcal{C}_{\max}$ and $\tilde{\delta}$. To translate this criterion into the curvature fluctuation ψ_0, we need to know the perturbation profile not only in the overdense region but also in the surrounding underdense region which may spread to large distances. We should also note that we do not expect that the profile-dependence parameters c_1, c_2 and c_3 strongly depend on the equation of state because these parameters are determined only by the initial density profile.

B. Uncompensated top-hat density model: Environmental effect

The physical argument about $\psi_{0,c}$ not only explains why neither $\tilde{\delta}_c$ nor $\mathcal{C}_{\max}$ but $\psi_{0,c}$ is significantly affected by the behavior of the surrounding region but also suggests that $\psi_{0,c}$ is affected by a significant environmental effect if the PBH formation results from a perturbation on top of a perturbation of longer wavelength. Such a situation is expressed in the top-hat density model by replacing the compensating underdense region with a perturbed region with the density perturbation δ_l. To describe the overdense region of scale r_0 with the density contrast δ_s surrounded by the perturbed region of scale σr_0 with the contrast δ_l, we generalize the top-hat density model given by Eq. (8.1) as follows,

$$\delta_{\mathrm{CMC}} = C_\delta[\Theta(r_0-r)+q\Theta(\sigma r_0-r)]\left(\frac{t}{r_0}\right)^{2-\frac{4}{3\Gamma}}, \tag{8.12}$$

where $q := \delta_l/\delta_s$. $K(r)$ is then given by

$$K(r) = \begin{cases} C_\delta'(1+q) & (0 \le r < r_0) \\ C_\delta'[(1+q)r_0^3+q(r^3-r_0^3)]/r^3 & (r_0 \le r < \sigma r_0), \\ C_\delta'(1+q\sigma^3)r_0^3/r^3 & (r \ge \sigma r_0) \end{cases}$$

$$\tag{8.13}$$

and C_δ' is given by Eq. (8.3). So this model has a nonvanishing mass excess and hence is uncompensated except for $q = -\sigma^{-3}$. We can identify r_0 and σr_0 with the short wavelength s and long wavelength l, respectively, so that $\sigma = l/s$. The phenomenological relations (8.10) should be replaced with

$$\psi_0 - 1 = \frac{3}{4}\frac{c_1}{c_2}\frac{1+q\sigma^2}{1+q}\mathcal{C}_{\max} = \frac{c_1}{c_3}\frac{3\Gamma+2}{8\Gamma}\frac{1+q\sigma^2}{1+q}\tilde{\delta},$$

$$\mathcal{C}_{\max} = \frac{c_2}{c_3}\frac{3\Gamma+2}{6\Gamma}\tilde{\delta}, \tag{8.14}$$

where we have introduced c_1, c_2 and c_3 to simply parametrize the profile dependence and nonlinearity. For the exact top-hat density model given by Eq. (8.12), we identify all of c_1, c_2 and c_3 with unity. Note that $\delta_l \ge -1$ if we assume the density field is everywhere nonnegative.

We should here note that to define $\tilde{\delta}$ we invoke averaging over the overdense region. However, if $\delta_l > 0$ in this model, the radius of the overdense region is not r_0 but σr_0. This is a subtle issue in the definition of the averaged density perturbation. We here continue to take r_0. In fact, if σ is much larger than unity, this ambiguity is rather in the choice of the averaging length. If we want to discuss the formation of black hole in the scale of r_0, we should make averaging with the scale of r_0.

Suppose that $q > -1$ and that $\mathcal{C}_{\max,c}$ and $\tilde{\delta}_c$ very weakly depend on the perturbations of longer wavelength. Equation (8.14) implies that $\psi_{0,c}$ is increased (decreased) when the overdense region of short wavelength scale r_0 is surrounded by an overdense (underdense) region of long-wavelength scale σr_0 with $\sigma > 1$ and $\delta_l > -\delta_s$. The larger the absolute value of the density perturbation ratio $|q|$ or the larger the scale ratio of the perturbations σ, the larger the environmental effect becomes. On the other hand, the requirement $K(r)r^2 < 1$ at $r = \sigma r_0$ implies that $q\sigma^2 \lesssim (1+q)\tilde{\delta}_c^{-1}$ for the threshold model in the case of $\sigma \gg 1$ and hence the environmental effect in $\psi_{0,c}$ remains of order unity if $q > 0$. On the other hand, if $q < 0$, that is, if the overdense region is located in a larger underdense region, there seems no limit on the environmental effect, although this must be interpreted with caution because the above estimate of ψ_0 only relies on the linear-order analysis. Hence, if one links the small value of $\psi_{0,c}$ to the efficient production of PBHs, one may conclude that the PBH production is significantly enhanced. It should be

noted that the above analysis is simplistic and further analysis is necessary in this context.

C. Top-hat curvature model: Sharpest transition

We can get an analytic expression for the top-hat curvature model, where $K(r)$ is given by

$$K(r) = \Theta(\Delta - r), \tag{8.15}$$

with $0 < \Delta \leq 1$. For $0 \leq r < \Delta$, we can find

$$\int_0^r \frac{dx}{x}\left(\frac{1}{\sqrt{1-K(x)x^2}} - 1\right) = -\ln\frac{1+\sqrt{1-r^2}}{2}. \tag{8.16}$$

Then, Eqs. (6.21) yield

$$\varpi = r\frac{1+\sqrt{1-\Delta^2}}{1+\sqrt{1-r^2}} \quad \text{or} \quad r = \frac{2(1+\sqrt{1-\Delta^2})\varpi}{(1+\sqrt{1-\Delta^2})^2 + \varpi^2} \tag{8.17}$$

for $0 < r < \Delta$ or $0 < \varpi < \Delta$, while $r = \varpi$ for $r \geq \Delta$ or $\varpi \geq \Delta$, and

$$\Psi^2 = \frac{1+\sqrt{1-r^2}}{1+\sqrt{1-\Delta^2}} \quad \text{or} \quad \Psi^2 = \frac{2(1+\sqrt{1-\Delta^2})}{(1+\sqrt{1-\Delta^2})^2 + \varpi^2} \tag{8.18}$$

for $0 < r < \Delta$ or $0 < \varpi < \Delta$, while $\Psi = 1$ for $r \geq \Delta$ or $\varpi \geq \Delta$.

Equations (4.68), (6.15) and (6.35) give $\delta_C, \tilde{\tilde{\delta}}_C$ and $\mathcal{C}_{\text{CMC}}$, where Eq. (6.20) gives

$$f = \Theta(\Delta - r) - \frac{\Delta}{3}\delta(\Delta - r). \tag{8.19}$$

The top-hat curvature model is clearly distinct from the top-hat density model because of the delta function in the density perturbation. This model is unphysical because the density perturbation δ is infinitely negative at the transition $r = \Delta$ from the overdense region to the FRW region. However, if the continuous model has a very sharp transition, then we expect that the top-hat curvature model may describe the dynamics of the continuous model approximately.

The top-hat curvature model has infinite density gradient and hence infinite pressure gradient force for general equations of state. Moreover, since the density perturbation itself is negatively infinite at the transition due to the presence of the delta function, the pressure gradient force always dominates gravitational attraction and hence prevent the model from collapsing to a black hole except for

the case in which the overdense region is initially trapped. This implies that the criterion for the black hole formation should be given by $K(r)r^2 = 1$ at the transition, i.e., $\Delta = 1$, because the coordinate singularity at which $K(r)r^2 = 1$ implies a marginally trapped surface [19]. This means $\tilde{\delta}_c = 3\Gamma/(3\Gamma + 2)$ and $\mathcal{C}_{\text{max},c} = 1/2$, respectively. The result of the numerical simulation by Polnarev and Musco [11] for the sharpest top-hat-type profile is consistent with this argument. If we substitute $\Delta = 1$ and $r = \varpi = 0$ into Eq. (8.18), we find $\psi_0 = \sqrt{2}$. This is close to $\psi_{0,c}$ for σ not so larger than unity as seen in Table I. The similar trend is also seen in Table II for the larger values of α. Since these models have a steeper transition from the overdense region to the FRW universe, our expectation is supported by the numerical result. That is, the threshold values for the model with a sufficiently steep transition will be approximately given by those for the top-hat model, $\tilde{\delta}_c = 3\Gamma/(3\Gamma + 2)$, $\mathcal{C}_{\text{max},c} = 1/2$ and $\psi_{0,c} = \sqrt{2}$.

D. Double top-hat curvature model: Environmental effect

Next we move onto a double top-hat curvature model, for which $K(r)$ is given by

$$K(r) = (1-A)\Theta(\Delta_1 - r) + A\Theta(\Delta_2 - r), \tag{8.20}$$

where A is constant, $0 < \Delta_1 \leq \Delta_2$ and we require $K(r)r^2 \leq 1$ for the avoidance of the coordinate singularity. A similar model is used in Nakama [16] in a different context [37]. We now extract an environmental effect from this simple model. For this model, Eqs. (4.68), (6.15) and (6.35) give $\delta_C, \tilde{\tilde{\delta}}_C$ and $\mathcal{C}_{\text{CMC}}$, where Eq. (6.20) gives

$$f = (1-A)\left[\Theta(\Delta_1 - r) - \frac{\Delta_1}{3}\delta(\Delta_1 - r)\right] + A\left[\Theta(\Delta_2 - r) - \frac{\Delta_2}{3}\delta(\Delta_2 - r)\right], \tag{8.21}$$

and from Eq. (6.18) we can find

$$\psi_0 = \sqrt{\frac{2(1+\sqrt{1-\Delta_1^2 A})}{(1+\sqrt{1-\Delta_1^2})(1+\sqrt{1-\Delta_2^2 A})}}. \tag{8.22}$$

We can see that the single top-hat curvature model is reproduced by putting $A = 0$ or $A = 1$ or $\Delta_1 = \Delta_2$. We can make identification $s = \Delta_1$, $l = \Delta_2$ and $q = \delta_l/\delta_s = A/(1-A)$, and hence the central overdense region is surrounded by the lower but still overdense region if $0 < A < 1$, while the surrounding region is underdense if $A < 0$. We should however note the delta function contributions in the density profile again.
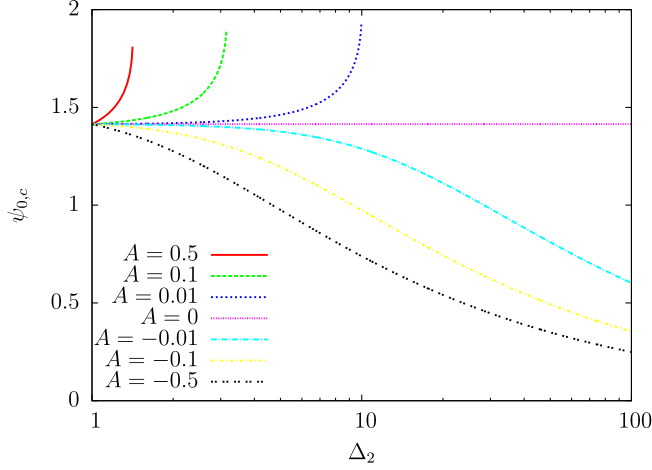
FIG. 4 (color online). The threshold values of $\psi_{0,c}$ for the double top-hat curvature model given by Eq. (8.20) as functions of Δ_2 with different values of A.

Similarly to the single top-hat curvature model, the threshold for black hole formation in this model is given by $\max(\Delta_1^2, \Delta_2^2 A) = 1$. Let us focus on the cases where $\Delta_2^2 A < 1$. Then, $\Delta_1 = 1$ gives a threshold and hence $\tilde{\delta}_c = 3\Gamma/(3\Gamma + 2)$ and $\mathcal{C}_{\mathrm{max},c} = 1/2$. Therefore, $\tilde{\delta}_c$ and $\mathcal{C}_{\mathrm{max},c}$ do not depend on the surrounding region. However, this is not the case for $\psi_{0,c}$, which is calculated as

$$\psi_{0,c} = \sqrt{\frac{2(1 + \sqrt{1 - A})}{1 + \sqrt{1 - \Delta_2^2 A}}}. \tag{8.23}$$

Figure 4 shows $\psi_{0,c}$ as a function of Δ_2 for different values of A. Noting $\Delta_2 > \Delta_1 = 1$ and $\Delta_2^2 A < 1$, we can conclude that $\psi_{0,c} > \sqrt{2}$ for $A > 0$, while $\psi_{0,c} < \sqrt{2}$ for $A < 0$. If $\Delta_2(> 1)$ is fixed, $\psi_{0,c}$ monotonically increases from $\sqrt{2/\Delta_2}$ to $\sqrt{2(1 + \sqrt{1 - 1/\Delta_2^2})}$ as A increases from $-\infty$ to $1/\Delta_2^2$. If $A \in (0, 1)$ and A is fixed, $\psi_{0,c}$ monotonically increases from $\sqrt{2}$ to $\sqrt{2(1 + \sqrt{1 - A})}$ as Δ_2 increases from 1 to $1/\sqrt{A}$. If $A < 0$ and A is fixed, $\psi_{0,c}$ monotonically decreases from $\sqrt{2}$ to 0 as Δ_2 increases from 1 to ∞. Thus, the existence of the surrounding overdense (underdense) region of longer wavelength increases (decreases) $\psi_{0,c}$ and, hence, suppresses (enhances) the PBH production if one assumes that the smaller $\psi_{0,c}$ is directly related to higher production rate. Moreover, the environmental effect on $\psi_{0,c}$ is bounded if the density perturbation of longer wavelength is positive, while $\psi_{0,c}$ even gets smaller than the unperturbed value if the wavelength l of the underlying negative density perturbation is sufficiently long and $q = \delta_l/\delta_s$ is fixed, and approaches 0 in the limit where l is infinitely long. The qualitative behavior of $\psi_{0,c}$ is common for both the uncompensated top-hat density model and the double top-hat curvature

model, in spite of the physical difference between the models.

IX. CONCLUSION

We have constructed cosmological nonlinear perturbation solutions with the long-wavelength scheme in the CMC, uniform-density, comoving and geodesic slicings without assuming symmetry. These solutions are generated by only a master variable $\Psi = \Psi(x^k)$, where the perturbations from the flat FRW solution can be arbitrarily large. We have also derived the explicit relation among these four slicings. One of the interesting applications is to construct initial data for primordial structure formation with and without spherical symmetry. For example, we can study nonspherical effects on the PBH formation, which are expected to be important especially for the soft equation of state.

Then, we have presented two distinct formulations of spherically symmetric spacetimes and the definitions of mass excess, compaction function and averaged density perturbation as spatial gauge invariant but slicing dependent perturbation quantities. Based on the general formulation of long-wavelength solutions, we have constructed spherically symmetric long-wavelength solutions in the CMC slicing and in the comoving slicing. We have elucidated the relation between the two spatial coordinates, the conformally flat coordinates and the areal radial coordinates. Using these solutions and relations, we have established the equivalence between the long-wavelength solutions given in Shibata and Sasaki [9] and the asymptotic quasihomogeneous solutions given in Polnarev and Musco [11], both of which have been used as initial data sets for the simulations of PBH formation.

Using this equivalence, we have reproduced the numerical simulation by Shibata and Sasaki [9] with the numerical code based on the formulation by Polnarev and Musco [11] and obtained the results which agree with the results of Shibata and Sasaki [9]. We have also calculated $\psi_{0,c}$ for the numerical simulation by Polnarev and Musco [11]. Combining these results, we have discussed that the smoother the transition from the overdense region to the FRW universe is, the smaller the $\tilde{\delta}_c$ and $\mathcal{C}_{\mathrm{max},c}$ become. The minimum values of $\tilde{\delta}_c$ and $\mathcal{C}_{\mathrm{max},c}$ are attained if the transition from the overdense region to the homogeneous universe is the smoothest. We have discussed that the analytic threshold formula obtained by Harada *et al.* [19] should apply for this case, while the analytic formula for the possible maximum value can be regarded as the threshold value for a sufficiently sharp transition. We have found the relation among ψ_0, $\mathcal{C}_{\mathrm{max}}$ and $\tilde{\delta}$ by using the compensated top-hat density model and interpreted why $\psi_{0,c}$ shows an apparently opposite behavior within the (approximately) compensated models to those of $\tilde{\delta}_c$ and $\mathcal{C}_{\mathrm{max},c}$. Moreover,

generalizing the top-hat density model to the uncompensated one, we suggest an environmental effect on $\psi_{0,c}$ from the underlying long-wavelength perturbations. This is also supported by the double top-hat curvature model, which can be treated in a fully analytic and nonlinear manner. We conclude that even if $\tilde{\delta}_c$ and $\mathcal{C}_{\mathrm{max},c}$ are not sensitive to the density profiles in the surrounding region, $\psi_{0,c}$ can be significantly larger (smaller) if the density perturbation of the wavelength in which we are interested is in the underlying positive (negative) density perturbation of much longer wavelength.

[1] Y. B. Zel'dovich and I. D. Novikov, Sov. Astron. **10,** 602 (1967).
[2] S. Hawking, Mon. Not. R. Astron. Soc. **152,** 75 (1971).
[3] B. J. Carr, Astrophys. J. **201,** 1 (1975).
[4] B. J. Carr, K. Kohri, Y. Sendouda, and J. Yokoyama, Phys. Rev. D **81,** 104019 (2010).
[5] B. J. Carr and S. W. Hawking, Mon. Not. R. Astron. Soc. **168,** 399 (1974).
[6] D. K. Nadezhin, I. D. Novikov, and A. G. Polnarev, Sov. Astron. **22,** 129 (1978).
[7] I. D. Novikov and A. G. Polnarev, Sov. Astron. **24,** 147 (1980).
[8] J. C. Niemeyer and K. Jedamzik, Phys. Rev. D **59,** 124013 (1999).
[9] M. Shibata and M. Sasaki, Phys. Rev. D **60,** 084002 (1999).
[10] I. Musco, J. C. Miller, and L. Rezzolla, Classical Quantum Gravity **22,** 1405 (2005).
[11] A. G. Polnarev and I. Musco, Classical Quantum Gravity **24,** 1405 (2007).
[12] I. Musco, J. C. Miller, and A. G. Polnarev, Classical Quantum Gravity **26,** 235001 (2009).
[13] I. Musco and J. C. Miller, Classical Quantum Gravity **30,** 145009 (2013).
[14] A. G. Polnarev, T. Nakama, and J. Yokoyama, J. Cosmol. Astropart. Phys. 09 (2012) 027.
[15] T. Nakama, T. Harada, A. G. Polnarev, and J. Yokoyama, J. Cosmol. Astropart. Phys. 01 (2014) 037.
[16] T. Nakama, J. Cosmol. Astropart. Phys. 10 (2014) 040.
[17] A. M. Green, A. R. Liddle, K. A. Malik, and M. Sasaki, Phys. Rev. D **70,** 041502 (2004).
[18] S. Young, C. T. Byrnes, and M. Sasaki, J. Cosmol. Astropart. Phys. 07 (2014) 045.
[19] T. Harada, C. M. Yoo, and K. Kohri, Phys. Rev. D **88,** 084051 (2013); **89,** 029903(E) (2014).
[20] Y. Tada and S. Yokoyama, arXiv:1502.01124.

[21] S. Young and C. T. Byrnes, arXiv:1503.01505.
[22] D. H. Lyth, K. A. Malik, and M. Sasaki, J. Cosmol. Astropart. Phys. 05 (2005) 004.
[23] A. G. Polnarev and M. Y. Khlopov, Sov. Astron. **25,** 406 (1981).
[24] A. G. Polnarev and M. Y. Khlopov, Sov. Astron. **26,** 391 (1982).
[25] M. Y. Khlopov and A. G. Polnarev, Phys. Lett. **97B,** 383 (1980).
[26] T. Suyama, T. Tanaka, B. Bassett, and H. Kudoh, Phys. Rev. D **71,** 063507 (2005).
[27] T. Suyama, T. Tanaka, B. Bassett, and H. Kudoh, J. Cosmol. Astropart. Phys. 04 (2006) 001.
[28] L. Alabidi, K. Kohri, M. Sasaki, and Y. Sendouda, J. Cosmol. Astropart. Phys. 09 (2012) 017.
[29] L. Alabidi, K. Kohri, M. Sasaki, and Y. Sendouda, J. Cosmol. Astropart. Phys. 05 (2013) 033.
[30] T. Nakamura, K. Oohara, and Y. Kojima, Prog. Theor. Phys. Suppl. **90,** 1 (1987).
[31] E. Gourgoulhon, arXiv:gr-qc/0703035.
[32] L. G. Jensen and J. A. Stein-Schabes, Phys. Rev. D **35,** 1146 (1987).
[33] M. Sasaki and T. Tanaka, Prog. Theor. Phys. **99,** 763 (1998).
[34] The corresponding expressions in Shibata and Sasaki [9] are slightly different, seemingly because of typos there.
[35] C. W. Misner and D. H. Sharp, Phys. Rev. **136,** B571 (1964).
[36] M. Kopp, S. Hofmann, and J. Weller, Phys. Rev. D **83,** 124025 (2011).
[37] Nakama [16] used a similar double top-hat curvature model to simulate the double formation of PBHs, in which the central perturbation first collapses and this is followed by another collapse of the larger perturbation swallowing the smaller PBH already formed.